A numerical framework to predict the performances of a tubular photobioreactor from operating and sunlight conditions

Ryma Laifa, Jérôme Morchain, L. Tiruta-Barna, Pascal Guiraud

A numerical framework to predict the performances of a tubular photobioreactor from operating and sunlight conditions.

Ryma Laifa, Jérôme Morchain, Ligia Barna, Pascal Guiraud

TBI, Université de Toulouse, CNRS, INRAE, INSA, Toulouse, France

Corresponding author: pascal.guiraud@insa-toulouse.fr

TBI, Université de Toulouse, CNRS, INRAE, INSA, Toulouse, France.

for any figures in print, color should be used.

Abstract

A framework model is proposed to evaluate the actual overall growth rate of microalgae in an outdoor tubular photobioreactor. A Monte Carlo-based radiative transfer modeling approach describes the local distribution of light energy inside the broth as a function of static (reactor geometry, location) and dynamic solar radiation parameters (angle of incidence, direct and diffuse solar contribution, incident radiation intensity). The light fields are coupled to a Lagrangian discrete random walk tracking of the cells to give the light variations experienced by each microalga for different broth flow rates. The cell light experiments are combined with a dynamic biological model to statistically calculate the actual overall growth rate. Using this model, 380 numerical experiments were performed for a wide range of geographic, light, biomass concentration, and broth flow turbulence conditions. Correlations for a *normalized* growth rate, Γ, relating the actual overall growth rate to its asymptotic behaviors (i.e., the instantaneous response and the full integration response), are proposed. The results clearly show that, for a fixed broth flowrate, Γ does not change with cell concentration variation. Under given light conditions, the level of turbulence linearly manages Γ, and thus the efficiency of sunlight utilization by the PBR biomass can be tuned by the broth flow rate in the tubular PBR. Γ also increases linearly with the diffuse fraction of solar radiation. A simple correlation is proposed for fast calculation of the actual overall growth rate.

Keywords

Tubular photobioreactor, Growth rate, Numerical experiments, Broth flowrate, Sunlight conditions.

39

40 Abbreviations

Latin letters			
a_z	Azimuth solar angle (°)	r	Tube radius (m)
D	Tube diameter (m)	Re	Reynolds number (-)
dt	Simulation step time (s)	t	Time (s)
dx	Elementary volume (m^3)	t_f	Integration time (s)
E_s	Mass scattering coefficient (m^2/kg)	T_L	Fluid Lagrangian integral time (s)
E_a	Mass absorption coefficient (m^2/kg)	U_b	Bulk flow velocity (m/s)
f	Function	$\bar{u}$	Mean longitudinal velocity (m/s)
g	Phase function coefficient (-)	$\acute{u}$	Longitudinal turbulent fluctuation (m/s)
i	Internal cell propriety (-)	$\acute{v}$	Radial turbulent fluctuation (m/s)
I	Global irradiance field (-)	V	Photobioreactor volume (m^3)
I_b	Direct irradiance field (-)	$\acute{w}$	Tangential turbulent fluctuation (m/s)
I_d	Diffuse irradiance field (-)	**X**	Biomass concentration (g/L)
I_0	Global incident irradiance value ($\mu mol.m^{-2}.\ s^{-1}$)	**(r,θ,z)**	Cylindric spatial coordinates
k	Turbulent kinetic energy ($m^2.\ s^{-2}$)	**(x,y,z)**	Cartesian spatial coordinates (m)
$\dot{m}_V$	Gain in mass per unit time over the entire volume	x	Spatial location
m_V	Mass over the entire volume		
Greek letters			
α	Contribution coefficient of the diffuse irradiance (-)	ν	Kinematic viscosity of the fluid
p	Probability density function in mass	τ	Microalgae constant relaxation time (s)

p_V	Probability density function in reactor volume	τ_t	Eddy characteristic lifetime (s)
Γ	the integration rate of fluctuating light	φ	Zenith solar angle (°)
ε	Viscous dissipation rate of turbulent kinetic energy ($m^2. s^{-3}$)		
μ	Specific growth rate (d^{-1})		
μ_t	Friction velocity (m/s)		
Indexes & Superscripts			
P-I	Relationship between light intensity and photosynthesis growth		
V	Photobioreactor volume		
p	Particle (microalgae)		
k	Event		
rms	Root-mean-square		
a	Actual (Real case)		
$< >_V$	Volume average		

41

1. Introduction

43 One of the emerging fields of application of microalgae, which has been growing steadily over the
44 last decade, is food and feed [1]. Due to their nutritional qualities, some microalgae (in particular
45 *Arthrospira Platensis* and *Chlorella Vulgaris*) are used as food and /or feed supplement, they are
46 marketed as dried powder or capsules but also as fresh raw biomass. In addition, there are a wide
47 variety of areas where microalgae could be a renewable bioresource, such as the cosmetics [2],
48 pharmaceutical [3] green chemistry (biofuels in particular) and water treatment industries [4].
49 Industrial production of microalgae requires a high-performance system in terms of "optimal"
50 growth and light conversion, which remains a challenge for processes operating in real outdoor
51 conditions with sunlight.

52 A wide range of technologies for outdoor microalgae production systems can be identified. They are
53 classified and qualified according to their type either open, such as raceways, mainly used for large
54 scale commercial production [5], or closed reactors called photobioreactors (PBR) which are more
55 attractive compared to the first ones. Indeed, they offer the advantage of a controlled reaction
56 condition and exist in a wide variety of designs depending on the production needs. In this context,
57 exhaustive analyses of the limitations and advantages of each PBR configuration were carried out,
58 the challenge being to design a closed system that is cost-effective, competitive and so efficient in
59 terms of biomass productivity [6]–[10]. From a performance point of view, there are more
60 arguments in favor of flat plan and tubular photobioreactors characterized by a high surface/volume
61 ratio and efficient sunlight harvesting that guarantee a good photosynthetic efficiency [11]–[13].
62 They are commonly used either outdoor in direct sunlight or in a greenhouse to possibly control
63 temperature and light. So far, there is no consensus on the ideal type of photobioreactor.

64 Predicting the performance of a solar photobioreactor requires an essential analytical approach
65 focused on radiative transfer, which allows a correct estimation of the light energy, brought by the
66 radiation, distributed in the volume and converted into biomass using mineral nutrients and water.
67 For outdoor systems, when all other physiological parameters are maintained at their optimal values,
68 the productivity of solar systems in any configuration is limited by sunlight, which varies over time

and according to the geographical position and orientation of the system. Therefore, it should be possible either to account for this incoming and outgoing energy or to obtain accurate information on what is happening in the reaction volume where this energy is used. With this in mind, detailed modelling approaches have been developed to evaluate outdoor solar PBRs based on the coupling of variable irradiance conditions (i.e. sunlight fluctuations intensity and the diffuse fraction of intercepted radiation) with photosynthetic growth kinetics [14]–[18].

Comprehensive and detailed models can provide a good simulation tool for solar systems despite their complexity. However, to the best of our knowledge, for the evaluation of photosynthetic growth rate, the aforementioned approaches focus on the instantaneous response of microalgae to local light. The latter is previously quantified by a light attenuation model either Beer-Lambert law or a two-flow model [19] which considers absorption without and with diffusion by microalgae respectively. Indeed, none of these simulations include the dynamic response of the cells to the light actually seen as they move along the light gradient, which allows to account for the effect of light/dark cycles called "flashing light" [20]–[22].

This effect, which is driven by the combination of mixing (large eddy scale and local turbulence) and spatial light heterogeneity, depends on bioreactor geometry. Experimental and modelling studies of lab scale illuminated PBRs for different species have frequently shown that mixing can induce a range of fluctuating light levels, with frequencies ranging from 0.05 to 50 Hz, while frequencies above 1 Hz can improve PBR performance [23]–[31].

Regarding the paramount importance of this rate of change in the light signal structure on the photosynthetic yield and consequently on the algae growth rate in PBR, in the last decade several numerical simulation studies have taken an interest in modeling the effect of coupling hydrodynamic, irradiance field and kinetics using different approaches. The latter were based on either direct numeric simulations [32], the integration of a dynamic kinetics of photosynthesis and the fluid dynamics [33], [34] or a stochastic Lagrangian approach for bubble column PBR [35], [36] and for tubular PBR [37], [38]. Other more or less complex approaches have been proposed [26], [39] [40], [41] to evaluate the performance of different photobioreactor configurations.

We note that a robust biological model is needed to properly describe the effect of light changes on the dynamics of photosynthesis. Some existing models involve internal metabolic processes acting at different time scales (i.e. photoinhibition and acclimatation) [27], [42]–[44]. These works are generally based on the concept of photosynthetic unit PSU initiated by Eilers & Peeters [45] and account for the dynamic response of photosynthetic processes with photoinhibition and recovery [46]. Despite their robustness, the application of these concepts for simulation requires the calibration of all model parameters for the species under study. Moreover, their computational accuracy is compromised by the wide range of spatio-temporal scales of kinetic and hydrodynamic phenomena involved in the process. Thus, this limits their use in large-scale modeling. Other dynamic models have also already been put forward in literature [47]–[50].

In the same line, Gernigon et *al.*, [35] proposed a first-order dynamic model to relate the algal response to light fluctuations in order to estimate the actual growth rate in a PBR. It considers the light history of the cells and introduces the internal physiological characteristics of the microalgae as a state variable. Their approach led to a simple expression for the photosynthetic rate, which is easily amenable to mathematical analysis under a quasi-stationary approximation. This model using a single-parameter (i.e. characteristic time) was easier to calibrate. Furthermore, it demonstrated its predictive capabilities for our strain of interest on the basis of several data from the literature [28], [51]. Therefore, to contribute to a continuing modeling effort of our research team, the present work is based on this model which has been experimentally validated and whose structure and mathematical properties are well established for a PBR illuminated by constant artificial light.

The main novelty of this paper is the extension of this coupling approach including fundamental investigations on: (1) the radiative transfer process, (2) Lagrangian cell tracking and (3) biological reaction dynamics, to calculate the actual performance (expressed as growth rate) in an outdoor tubular using variable sunlight. Specifically, massive simulations of 380 possible cases were performed to consider various photo-process parameters such as biomass concentration, flow rate of the culture medium as well as the characteristics of solar energy: direct sunlight incidence angles, diffuse light fraction and their intensities. The results of these numerical experiments were correlated to the investigated macroscopic parameters in order to provide a fast estimation of the growth rate. Indeed, the progression from the microscopic scale to the process scale is the key point

of this work. The ambition being later to be able to use this growth rate model correlation to foresee the productivity over a full year, at any place on earth, using geo-located weather data and operating conditions of the PBR investigated.

2. Modeling approaches

2.1. Methodology

The core of our approach lies in accessing the distribution of "light conversion efficiency" in the algae population. Basically, in culture volume, light is spatially heterogeneous due to absorption and scattering by microalgae. Therefore, in a stationary light field, flow-transported cells are exposed to a fluctuating light signal to which they respond dynamically. The features of this signal result from the convolution of the stationary light field and the cell's velocity and location. The latter are calculated using a Discrete Random Walk model along with the known turbulent flow velocity profile (detailed in section 2.3). To establish the light field, a rigorous light transfer simulations were carried out using a Monte Carlo homemade algorithm including relevant parameters such as the PBR geometry, its wall's characteristics (refraction, reflection, and transmission), and microalgae's radiative properties (model description in section 2.2).The combination of these two independent fields determine "the rate of light change along the cell trajectory".

Microalgae are known to adopt a growth rate which is related to the integral of the light received over a defined time scale. Thus, microalgae are not at equilibrium with their local environment. In other words, their actual growth rate μ_V^a is not set by the average intensity received by the cells (defined as full light intensity integration i.e. $\mu(\langle I \rangle_V)$), nor by the local light fields as an instantaneous response (no light intensity integration i.e. $\langle \mu(I) \rangle_V$) but must include the previously encountered light signal in a recent past (defined by the above-mentioned integration time scale). This fact has been identified and reported by Terry in 1986 [22], who introduced the concept of "The proportional light integration" :

$$\Gamma = \frac{\mu_V^a - \langle \mu(I) \rangle_V}{\mu(\langle I \rangle_V) - \langle \mu(I) \rangle_V} \quad (1)$$

This *normalized* specific growth rate, Γ, is observed and measured experimentally. However, there is no predictive method to quantify the actual growth rate and its departure from asymptotic cases namely (no or full light intensity integration). We propose to predict this quantity μ_V^a from the local

153 distribution of individual cell capacity to convert light. In line with previous works, we name this cell
154 property, i, we assume that the microalgae population is segregated according to this property and
155 put that microalgae characterized by i are able to grow at $\mu(i)$. The relationship $\mu = f(i)$ is known
156 as "P-I relationship" describing the inherent link between constant light intensity I and
157 photosynthesis P (see **Appendix A**).

158 If we now define the probability density function in mass $p(\boldsymbol{x}, i, t)$ such that $p(\boldsymbol{x}, i, t)di$ is the mass
159 fraction of algae with their property $i \in [i, i + di]$ at location $\boldsymbol{x}$ at time t. The local, actual,
160 population averaged specific growth rate $\mu^a(\boldsymbol{x}, t)$ in mass, obeys the following definition:

$$\mu^a(\boldsymbol{x}, t) = \int_0^\infty \mu(i) p(\boldsymbol{x}, i, t) di \tag{2}$$

161

162 Introducing the local concentration of algae, $X(\boldsymbol{x})$, as the total mass of algae in that elementary
163 volume $d\boldsymbol{x}$, the gain in mass per unit time over the entire volume of the reactor is retrieved from a
164 volume integration. The resulting growth rate at the reactor scale is

$$\mu_V^a = \frac{\dot{m}_V}{m_V} = \frac{\int_V X(\boldsymbol{x}) \int_0^\infty \mu(i) p(\boldsymbol{x}, i, t) di \; d\boldsymbol{x}}{\int_V X(\boldsymbol{x}) d\boldsymbol{x}} \tag{3}$$

165

166 Thus, the major difficulty in calculating the actual growth rate at the reactor scale comes from
167 determining the cell property distribution $p(\boldsymbol{x}, i, t)$. Indeed, the cell spatial distribution is uniform
168 (cell iso-density is validated in section 3.2.2) so that the actual specific growth rate becomes:

$$\mu_V^a(t) = \frac{1}{V} \int_V \int_0^\infty \mu(i) p(\boldsymbol{x}, i, t) di \; d\boldsymbol{x} \tag{4}$$

169

170 Interestingly, the same quantity can also be expressed using the distribution of cell property at the
171 reactor scale, $p_V(i, t)$

$$\mu_V^a(t) = \int_0^\infty \mu(i) \frac{1}{V} \int_V p(\boldsymbol{x}, i, t)\, d\boldsymbol{x}\, di \; = \int_0^\infty \mu(i) p_V(i,t) di \tag{5}$$

172

173 In this work, the distribution $p_V(i,t)$ is approximated by the probability to find a cell with the
174 property i, whatever its location.

$$p_V(i,t) = \frac{N(i,t)}{\sum N(i,t)} \tag{6}$$

175

176 Hence, the problem is solved by tracking the location of a large number of particles while adapting
177 their internal property i. In our previous modelling works, a relaxation model was proposed and
178 experimentally validated for a more realistic prediction of the PBR performances [35]. This non-
179 equilibrium model reflects this dynamic biological adaptation of microalgae to surrounding light
180 fluctuations. According to [35], each cell is characterized by an internal propriety defined as its light
181 conversion efficiency, *i*, that tends towards the local light experienced by cell, $I(x)$, and it is given by:

$$\partial i / \partial t = \; 1/\tau \,.\, (I(\boldsymbol{x}) - i) \tag{7}$$

182

183 with $\tau = 0.3\ s$ being the microalga relaxation time constant which has been calibrated on the basis
184 of fairly recent experimental data [28], [35]. This model enables description of the effect of flashing
185 light frequency on the global growth rate**.** It has already demonstrated its reproducibility and
186 success for a wide range of light frequencies (i.e. several durations of day/night cycle).

187 From a calculation point of view, to compute the actual overall growth rate, the integration method
188 chosen is to sum over a large number of Lagrangian particles $N_p$and over N_k consecutive sampling
189 time events (Monte Carlo) until the initial condition $N_p(i,0)$ is forgotten, i.e. the ensemble average is
190 constant.

$$\mu_V^a = \frac{1}{N_p\, N_k} \sum_{p=1}^{N_p} \sum_{k=1}^{N_k} \mu(i) \tag{8}$$

From Eq.(4) and Eq.(7), it is straightforward to show that if the response time to light fluctuations is infinitely small $p(\boldsymbol{x}, i, t) = \delta(i - I(\boldsymbol{x}, t))$ which means that all cells at $\boldsymbol{x}$ are in the same state $i = I(\boldsymbol{x}, t)$. This case is commonly referred as instantaneous response.

$$\mu^{a}_{V,\tau\to 0} = \frac{1}{V}\int_V \int_0^{\infty} \mu(i)\delta\big(i - I(\boldsymbol{x}, t)\big)di \; d\boldsymbol{x} = \frac{1}{V}\int_V \mu\big(I(\boldsymbol{x}, t)\big)d\boldsymbol{x} = \langle \mu(\boldsymbol{I})\rangle_V \qquad (9)$$

Similarly, if the response time to light fluctuation is infinite, $p(\boldsymbol{x}, i, t)$ become independent of the spatial coordinate is $p(\boldsymbol{x}, i, t) = \delta(i - \langle I\rangle_V)$. This case is commonly referred as full integration.

$$\mu^{a}_{V,\tau\to \infty} = \frac{1}{V}\int_V \int_0^{\infty} \mu(i)\delta(i - \langle I\rangle_V)di \; d\boldsymbol{x} = \frac{1}{V}\int_V \mu(\langle I\rangle_V)d\boldsymbol{x} = \mu(\langle \boldsymbol{I}\rangle_V) \qquad (10)$$

These two asymptotic responses patterns (9) and (10), can be obtained by a direct coupling between the irradiance field results and the growth kinetic model without considering actual cell trajectories and cell capacity to convert light.

The sketch in **Fig. 1**. summarizes the modeling methodology undertaken in this study to compute the overall growth rate in tubular PBR then deduce the value of *normalized* specific growth rate, Γ, using the two asymptotic cases mentioned above.

This approach is applied to a horizontal tube (considered as the model element of a tubular PBR) operating under a range of dynamic functioning conditions such as biomass concentration and light energy, which vary in time and according to the plant geographic position.

The key point of this work is to describe Γ as a function of the studied operating parameters and thus theoretically infer the actual overall growth rate. Thus, a burst of 380 simulations were performed to sweep a wide range of operating cases, then Γ were correlated to the main parameters.

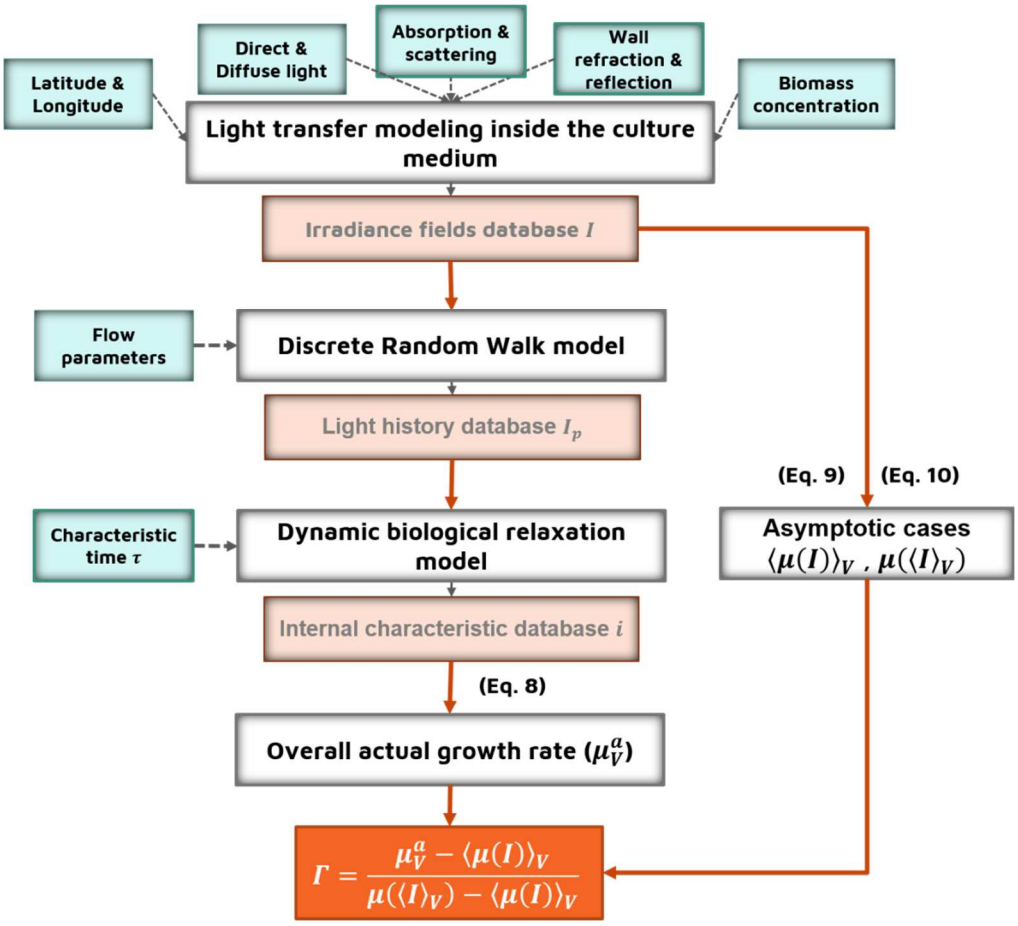

211

212 **Fig. 1.** Diagram of the modelling approach. Green box: input parameter; Grey box: modeling

213 method. Pink box: results database

214

2.2. Local available light inside solar tubular PBR

As the light is the main parameter affecting the growth of autotrophic microalgae, properly quantifying the local distribution of light within the PBR is important, especially when the irradiance heterogeneities are striking. In this section, the aim is to simulate the light distribution in the suspension as a function of the variable solar radiative flux, in a defined location.

Unlike many existing models that often rely, in their calculation of the overall photosynthesis rate, on the incident or average light intensity reaching the culture [52], [53], we rigorously describe the propagation and distribution of sunlight (composed of direct and diffuse fractions) in the whole volume.

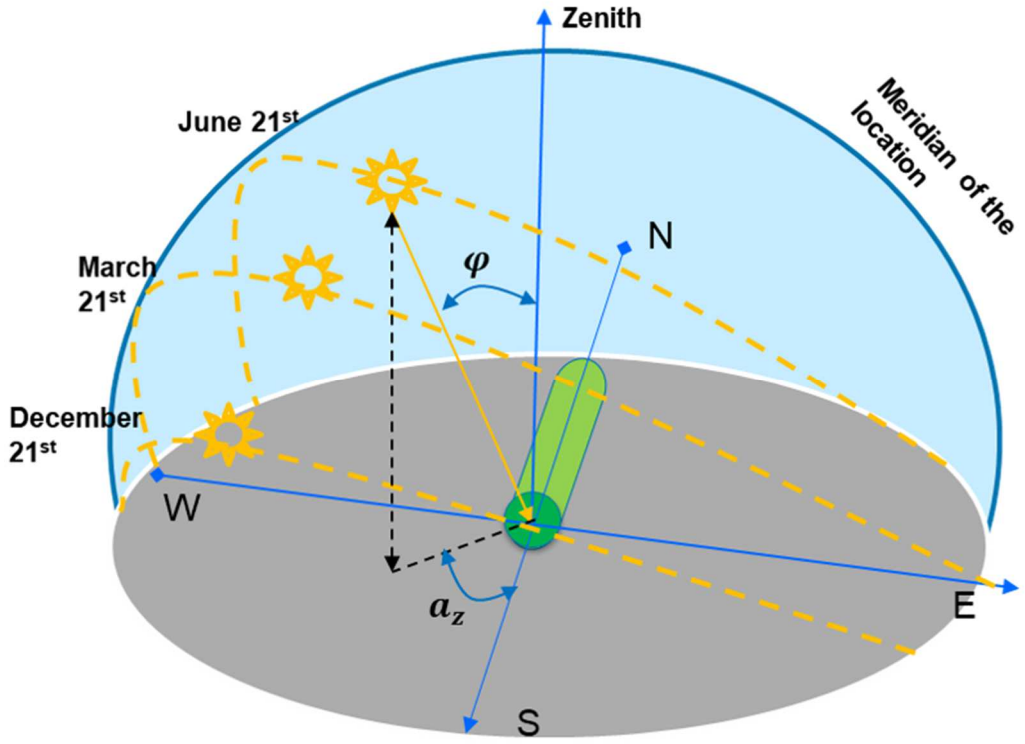

Fig. 2. Diagram of sun's position angles and orientation of a tubular PBR

The sun's apparent position is described by two main angles zenith (φ) and azimuth solar (a_z) as shown in **Fig. 2.** These angles are calculated using equations from literature [54], which include the geographic localization (latitude & longitude) of the site, the day in the year and the time.

For an outdoor tubular cultivation system, the maximum flux collected during the sun course is obtained when the tube is aligned on a north-south axis, this orientation was chosen.

Our model includes these particular characteristics in the representation of: (i) the non-normal incidence of direct sunlight on the PBR surface that drives the photon entrance and propagation within the reactor, and (ii) the hourly and annual variation of the levels of diffuse irradiation and the flux density of the direct incident light. An appropriate OXYZ photon moving marker was defined for characterizing the incident light direction by two new angles (Ψ) and (θ), which are expressed as a function of zenith (φ) and azimuth (a_z) solar angles. The formulae used and the corresponding diagrams are presented in supplementary document (**Appendix B.1**).

Because of the complexity in solving the RTE (The integro-differential Radiative Transfer Equation) analytically or even numerically when all phenomena are included, some approaches based on approximations can be found in the literature. For example, [56]–[58] used an analytical solution based on a one-dimensional approximation of scattering known as the Two-flux method. In this approach, only the forward and backward propagation directions are considered, which corresponds to two diffuse radiation flows propagating inwards and outwards from the medium. Among the approximate analytical models, the P1 approach (assuming that energy is distributed uniformly over all directions) was proposed to solve the RTE in solar tubular photocatalytic reactors [59]. However, others studies have used numerical methods of resolution as the finite volume method [60], the discontinuous Galerkin method [15], and Monte Carlo method applied for a plane-slab photocatalytic reactor [61] or for different PBR geometries [62]–[64].

The simulation of the local irradiation field in solar PBR tubes should consider the corresponding light energy balance including: the transmission, absorption, diffusion in the algal broth, as well as the illuminated surface geometry (curvature of the walls). Previous works on the same PBR design neglected the light scattering by cells (light multiple diffusion) and used only Beer-Lambert law to estimate the internal attenuation of light [14], [17], [65]. In contrast to these studies, here the Monte Carlo method is employed as a suitable approach for multi-phenomena modeling (details about this method in [66]). In this technique, events are considered corresponding to the following physical phenomena: (i) the deviation of the photon path due to its reflection/refraction by the PBR

wall according to Snell-Descartes laws, (ii) the energy fraction carried towards the culture by reflection or transmission according to Fresnel laws, (iii) the absorption in the culture broth according to Beer-Lambert's laws, and (iv) the anisotropic multiple diffusion (i.e. diffraction effects) due to the interaction with the cells using the phase function [67] (see formula in **Appendix B.2**).

Since the nature of incidence between direct and diffuse light is different, the corresponding irradiance fields are calculated separately. Indeed, the PBR is considered to receive parallel direct light rays on the upper hemicylindrical wall exposed to the sun, whereas the diffuse component of sunlight is assumed to have an isotropic Lambertian incidence. The diffuse light can come from any direction over the entire pipe wall (random propagation trough space). The global irradiance field I corresponding to the sunlight is finally calculated by the sum of the contributions resulting from each spatial distribution for direct I_b and diffuse I_d radiation:

$$I(x,y,z) = I_0 \times [\alpha \times I_d(x,y,z) + (1-\alpha) \times I_b(x,y,z)] \quad (11)$$

where a is the diffuse light contribution fraction and I_0 is the global incident light intensity.

To reduce the calculation cost and achieve a good simulation accuracy, it was found that a 2D matrix discretized with a square mesh of 10^6 segments, and about ten million photon's trajectories, were necessary to obtain the convergence of the calculation and a satisfactory representation of the light distribution field. The model was implemented and simulations are performed using MATLAB R2017b software (Mathworks) thanks to parallelization option to span the various cases of irradiance fields simultaneously. The developed model based on Monte Carlo approach was validated using analytical models for different simplified cases (detailed results in **Appendix B.3**).

2.3. Lagrangian study of cell transport in the pipe

In addition to the irradiance field determination, it is important to simulate the individual cell trajectories driven by the carrier fluid flow in the PBR. As the light field is identical all along the

tubular reactor axis, only the radial and azimuthal microalgae movements change the light intensity they experience along their trajectory. These radial and azimuthal cell movements are generated by turbulence and wall ejections. The most complete and accurate approach for this situation would be the direct resolution of the Navier-Stokes equations DNS (Direct Numerical Simulation) or using LES (Large Eddy Simulation). However, their implementation is limited by the computational costs because it requires discretization in very small time and space steps in order to capture all the structures of the turbulence. Thus, the added value of such a complex simulation can only be justified if the fine details of the trajectories are of great importance. The particle trajectory in a RANS-based flow simulation very often refers to a discrete random walk model. In the present work, the modelling relies on a Lagrangian cell tracking method based the algal trajectories from well-known 1-D turbulent flow profiles. In this case, a discrete random walk model provides a time-saving approach. Indeed, For a flow in a tube at different Reynolds numbers, the time required to perform an advanced CFD simulation as proposed in several studies[26], [29], [35], [69], [70], could take months, whereas the proposed approach takes only a few minutes

Only the radial and azimuthal velocity fluctuations are involved to produce the cell movement in the light field. They can be represented by two root-mean-square (RMS) components (v_{rms} et w_{rms}) transversal to the main flow. A collection of some experimental and numerical data from the literature was used to observe and analyze these velocity fluctuations in turbulent flows in a horizontal pipe. **Fig. 3.** presents the profiles of the ratios of the radial and azimuthal RMS variances by the friction velocity μ_T corresponding to different case studies [71], [72]. This figure indicates that these two non-dimensional fluctuating velocities are almost similar regardless of the Reynolds number, namely 17800, 24600, 38000 and 44000. In addition, their values remain almost maintained in the inner region of the tube until the beginning of the viscous sub-layer where they start to progressively decrease. Indeed, the turbulence tends towards the isotropy in the pipe center and presents an increasing anisotropy towards the boundary layer whose thickness varies with Reynolds number. However, the two transverse fluctuations keep similar values. This reproduces the classical behavior of a turbulent single-phase flow in a cylindrical pipe, which has been widely studied for a long time [73]–[76].

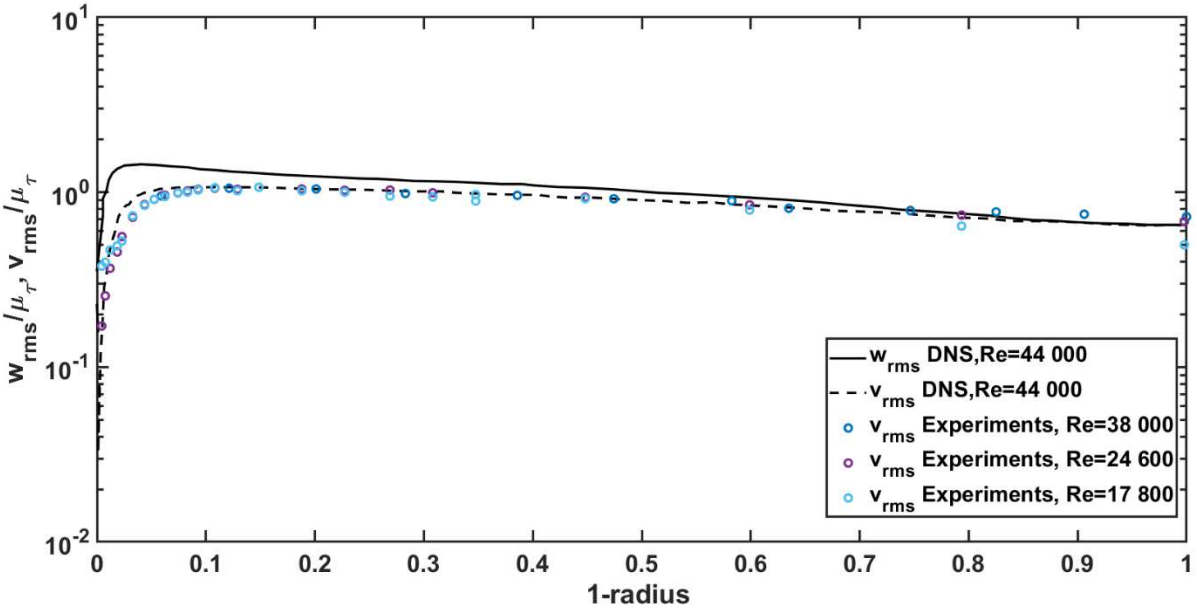

312

313 **Fig. 3**. Profiles of radial and tangential RMS components normalized by the friction velocity for
314 several Re resulting from experimental data [71] and numerical works [72].

315 Based on this, in our cell tracking the two transverse components of standard deviation values of the
316 fluid velocities (RMS velocities) are supposed to be equal and constant over the section.
317 Furthermore, these fluctuation values can be deduced from the one obtained at the center of the tube
318 where the turbulence is isotropic. To attain this value, calculation of turbulence in the continuous
319 phase has to be performed.

320 Some hypotheses have been considered: (i) the carrier fluid is assumed to be incompressible and
321 Newtonian, and (ii) cells have a small size and a density equivalent to that of the continuous phase.
322 Thus, they are considered as fluid particles that follow the flow lines without impacting the
323 continuous phase flow.

324

325 Numerical resolution of the continuity and Navier-Stokes equations was performed using the $k-\varepsilon$
326 model (RANS approach).
327 The most faithful modeling of the irregularity and random characteristics of turbulent flow should
328 be able to capture the details of turbulence diffusion due to vortex structures which is the main
329 mechanism of particle dispersion in the fluid. Taylor [77] introduces the concept of turbulent

diffusion for the modeling of the transport of passive particles by proposing a stochastic model coupled to a Lagrangian approach for a statistically stationary isotropic homogeneous turbulent flow.

The trajectories of particles are governed by a part related to the mean flow of the continuous phase and another part related to the action of the turbulence structures driven by the instantaneous fluctuations. It is therefore necessary to integrate the trajectory equation by using the instantaneous velocity components seen by the particle during their movements which, in the case of a horizontal pipe, are written in cylindrical coordinates such as:

$$\begin{aligned} u_z(t) &= \bar{u} + \acute{u}(t) \\ u_r(t) &= \acute{v}(t) \\ u_\theta(t) &= \acute{w}(t) \end{aligned} \tag{12}$$

With $\bar{u}$ the average longitudinal velocity and $\acute{u}(t)$, $\acute{v}(t)$, $\acute{w}(t)$ are the components of the instantaneous longitudinal, radial and tangential fluctuating velocities respectively.

For a more realistic simulation of the fluctuating part, a stochastic approach was used here via a discrete random walk (DRW) model, initiated by Hutchinson et *al.*, [78] for the study of particle dispersion in the turbulent flow field.

The DRW model assumes that a particle interacts with a sequence of vortices that are characterized by a time interval of interaction τ_t and random velocity fluctuations that are kept constant during this time. The principle is that once this interaction time has elapsed, a new random fluctuation independent of the previous one is introduced to account for an interaction with a new vortex. This characteristic time is known as "The characteristic lifetime of the eddy" and is defined as a constant given by local characteristics of the turbulent flow k and ε:

$$\tau_t = 2 \cdot T_L \tag{13}$$

$$T_L \approx 0.15 \cdot \frac{k}{\varepsilon} \tag{14}$$

With T_L "the fluid Lagrangian integral time"

The fluctuating velocities are randomly sampled in a normal distribution of zero mean and standard deviation equal to the RMS value of velocity fluctuations Eq.(15). Assuming that the turbulence is isotropic at the tube center, the RMS at any point in the flow is written as a function of the local

$$v' \sim N(0, v'_{rms}) \tag{15}$$

turbulent kinetic energy as follows:

$$u'_{rms} = v'_{rms} = w'_{rms} = \sqrt{(2k_c/3)} \tag{16}$$

k_c being the kinetic energy in tube center.

The time step chosen for our simulation is dt =0.05 (s). This value is set so that it is equal or inferior to the vortices lifetime in the tube center (resulting from considerations postulated in the previous paragraph) ranging from (0.09-0.44 (s)) for the case studied. This choice of time step is also made by respecting on one hand the classical conditions allowing an acceptable numerical stability of the solution with a lower cost of calculation time, and on the other hand the frequency range of the sampled irradiance signals (i.e. 20 Hz), thus, a good integration of the events undergone by the cell over its biological relaxation time τ =0.3 (s).

The particles positioning (r,θ,z) is calculated as follows:

$$\begin{cases} R_{T+DT} = R_T + u_r\,(t) \cdot dt \\ \Theta_{T+DT} = \Theta_T + u_\theta\,(t) \cdot dt \\ Z_{T+DT} = Z_T + u_z\,(t) \cdot dt \end{cases} \tag{17}$$

Using Lagrangian approach provokes a preferential trapping of particles next to the walls of the PBR. This is due to the assumption that turbulence is isotropic everywhere in the bulk, however, in the parietal zone, the turbulence is neither homogeneous nor isotropic as observed previously in **Fig. 3.** where the radial component of the velocity is smaller than the tangential one. As a result, the particles in the turbulent boundary layer are decelerated significantly and are not returned to the

372 flow. The calculated radial fluctuations in the vicinity of the wall are not sufficient to generate the
373 return of the particles inside the flow and so the continuity equation for the particle phase is not
374 respected. This numerical problem has also been raised by several CFD simulation studies using the
375 Lagrangian method to track particles in different types of PBR [26], [35], [69], [70].

376 As it is not possible to reproduce numerically the turbulent structures called "Bursting" present in
377 the boundary layer using $k-\varepsilon$, (only DNS approach could do that), we tried to overcome this
378 problem of accumulation by managing the particle wall ejection by their rebounds. The objective is
379 to ensure that the concentration of particles in the cross-section respects as well as the continuity
380 equation, i.e., their concentration keeps homogeneous since there is no phenomenon concentrating
381 them somewhere in the flow. The principle is to eject low velocity particles from the viscous sub-
382 layer into the internal flow. The particle rebound is managed by an adapted rebound coefficient. The
383 homogeneity of the cell's concentration will be checked later (section 3.2.2).
384
385 About one hundred thousand trajectories were simulated to form a statistically representative sample
386 of numerous paths taken by the cells. The particles are initially sampled in the entrance cross-section
387 of tube to ensure their homogenous distribution since the PBR is considered perfectly agitated.

3. Results and discussions

The model is designed with the aim of simulating the dynamic evolution of the light distribution in whole-year, outdoor running, PBR. Time varying parameters are: cell concentration (in the case of batch reactor), direct light incident angles, global incident irradiance, fraction of diffuse radiation.

The study case is a horizontal tubular PBR represented by a single isolated pipe with a diameter of D=0.05 m, and the broth medium containing the strain of species *Arthrospira platensis* (Spirulina). The list of physical quantities and parameters used for the simulations (model inputs) are presented in **Table 1.**

Table 1.

Model inputs for the application case (spirulina culture in a tube in thin poly-methyl methacrylate PMMA)

Parameter	**Values**	**Reference**
System orientation	North- South	-
Incidence light angles (a_z, φ)	Variable*	
Contribution coefficient of the diffuse irradiance α	Variable*	[55]
Global incident irradiance I_0	Variable*	[55]
Day of year	Variable*	-
	Variable*	-
Mass scattering coefficient E_s	640 (m^2/kg of dry Spirulina)	[58]
Mass absorption coefficient E_a	162 (m^2/kg of dry Spirulina)	[58]
Phase function coefficient g	0.97	[67]
Air refractive index n_{air}	1	
Refractive index of the broth n_{broth}	1.34	[35]

PMMA refractive index n_{PMMA}	1.49	[79]
Tube diameter D	0.05 (m)	-
Wall thickness	0.004 (m)	-
Biomass concentration	0.3-1.5 (g/L)	-

*Variable value depends on location, day and time.

We have tried to scan a range of representative flow velocities at typical velocities in tubular PBRs used at the technical scale [80], [81] to test the effect of turbulence on performance. **Table 2** summarizes the different parameters of the conditions tested in this work.

Table 2.

Details on the turbulent flow conditions in the pipe investigated

Flow Velocity U_b (m/s)	Re (U_b.D/ν)	μ_t (friction velocity)
0.3	15000	0.0179
0.4	20000	0.0231
0.5	25000	0.028
0.7	35000	0.0376
1.68	84000	0.0791

3.1. Light field in tubular PBR

Since the direct light characteristics vary over time, the range of possible values of Zenith and Azimuth angles was considered in order to represent several times of the day and in year. Therefore, using the symmetrical profile of the sun's path, it was possible to select a limited number of cases. Ten irradiance fields are calculated for cell concentrations ranging from 0.3 to 1.5 (g/L). Hence, 280 cases were performed. Not all results for irradiance field simulation for selected cell concentrations and sun positions, are presented here.

The fields are presented in normalized form with respect to the energy received in each illuminated elementary surface (i.e. divided by the number of photons used in simulation and the area of the mesh). Due to the invariance along the horizontal axis of the tube, the geometry is reduced to cross-section. Therefore, the results are the projections of the 3D motion of the photons in the volume onto this cross-section.

Only one example is shown here, a representative case of a typical summer day in Toulouse, France (43.36° N, 1.26° E) at solar noon where the Zenith angle $\vartheta = 20°$, Azimuth angle $a_z = 0°$ and diffuse fraction α=0.38. The irradiance fields with 1 (g/L) of biomass for the direct and diffuse solar radiation are shown in **Fig. 4**. (**a)** & **(b)** respectively and **Fig. 4**. (**c)** presents the total distribution of sunlight received on the culture.

As can be seen, there is a striking spatial heterogeneity of light distribution, hence, a significant difference is noticed between the regions close to the wall and those in the center of the tube **Fig. 4**. This is a specific feature usually mentioned in the literature for light-limited PBRs, and which is due to the absorption and scattering of light in the medium. Furthermore, the effect of the refraction and reflection of direct collimated light on the wall is clearly seen in **Fig. 4**. (**a**). Thus, due to the incurved surface, direct sunlight passing through the PBR interface is subject to a redirecting effect and obeys Fresnel's laws. As a result, the fraction of energy transmitted into the reactor volume is less than the solar energy arriving at the surface. This explains the non-uniform distribution of irradiation in the area near the illuminated surface (i.e. the hemisphere facing the sun). This feature has been also observed in [65]. The diffuse light irradiance field shown in **Fig. 4**. (**b)** is only concentration

dependent. Since this part of radiation is isotropic, the light come from any direction and it is better distributed than direct light over the entire wall of the pipe. However, compared to the overall field, the diffuse light field seems not significant even if its contribution is α=0.38.

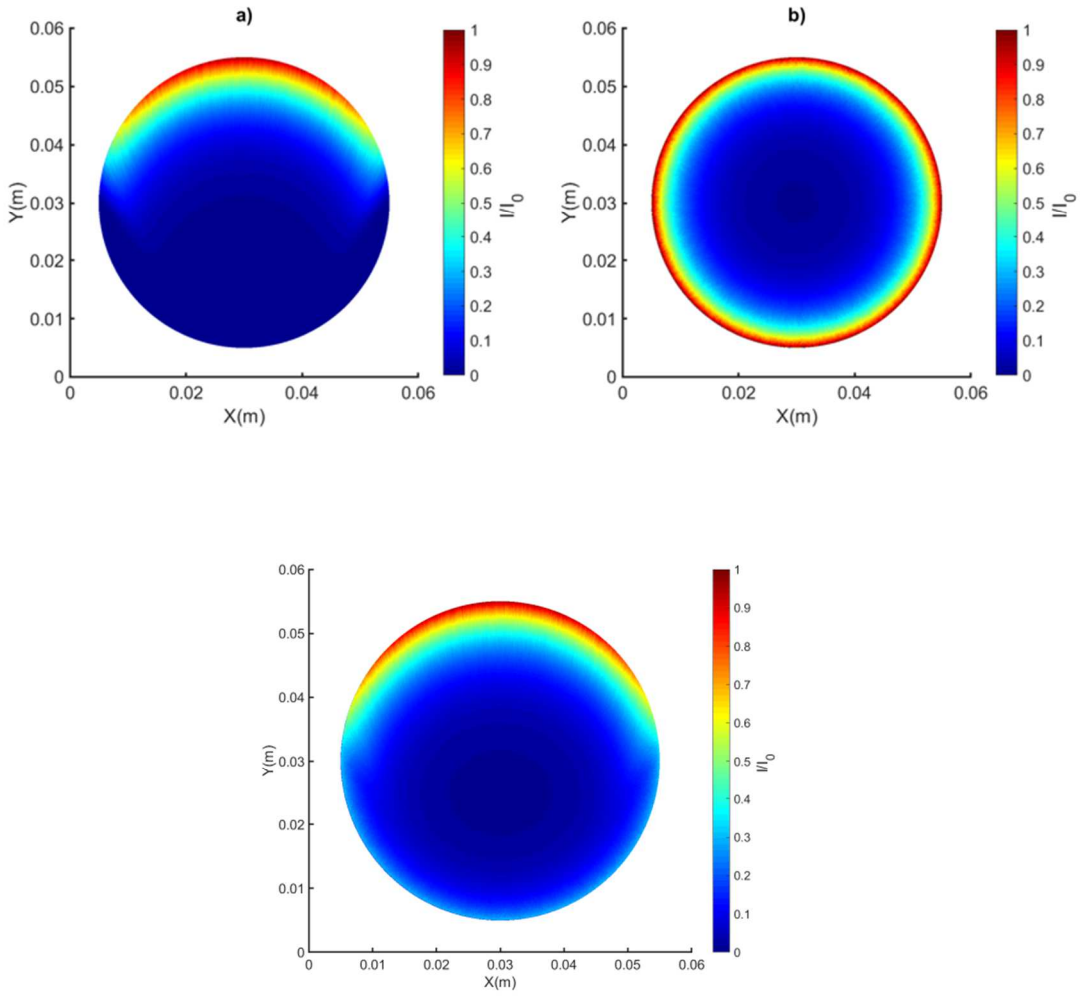

Fig. 4. Normalized local irradiance fields at biomass concentration X=1(g/L): (**a**) for direct sunlight with ϑ= 20° a_z=0°, (**b**) diffuse sunlight, (**c**) the sum of the contribution of the two fields direct and diffuse for solar midday of summer day in Toulouse diffuse coefficient α=0.38.

The irradiance distributions computed will be then multiplied by the global incident irradiance value I_0 corresponding to the investigated case, derived from the PVGIS data. The results for the selected

cell concentrations and sun positions constitute a data set to be combined with other modeling approaches in order to be exploited for photosynthetic growth calculation.

With an appropriate adaptation of the model, this approach can be applied to (i) other PBR geometries (e.g. rectangular or flat PBR), and (ii) other types of surface or volume lighting (e.g. artificial LED). Cell spatial distribution

3.1.1. Cell trajectories and their combination with the irradiance field

The goal here is to obtain data on the history of each cell exposure to light in order to further ~~exploit~~ use it in the estimation of overall growth rate. A collection of various trajectories was acquired using the method of sampling cell movement in the reactor described above (subsection 2.3). The interaction between hydrodynamics and light transfer is highlighted here. To ensure the statistical convergence of numerical resolution and to guarantee a meaningful representation of all possible events that microalgae undergo in PBR, a choice of 1.5×10^5 particles to be simulated, for a duration of 5s and with a time step of 0.05 (s), were deemed necessary to generate sufficient amount of information (i.e. about 10^7 events).

An example of trajectory recorded for an individual cell is illustrated in **Fig. 5** for a given hydrodynamic conditions (a flow velocity of 0.4 (m/s) corresponding to Reynolds number of 20000) over 5s of simulation. The main point of interest in this investigation is shown in **Fig. 5.(a)** which describes the bidimensional motion of the particle in the cross section of the tube where the light gradient occurs. These radial transitions projected in 2D plan effectively reproduce the stochastic aspect of the cell displacement predicted by the random walk model. These purely random redirections enable the capture of all light variations due to the turbulence, i.e. the local fluctuations characterizing the local eddies established in this type of flow. **Fig. 5(b)** illustrates the real-time tracking of the same particle where the radial movement is depicted along the longitudinal axis in 3D Cartesian coordinates. This database of the consecutive cell positions is then coupled directly with a given irradiation field (e.g. simulated for a concentration of 0.9 (g/L) and lighting conditions of a typical summer day in Toulouse at 10h solar time where α=0.4). Hence, the temporal light

regime seen by microalgae is recorded over 5 (s) with frequency of 20 (Hz) as represented in **Fig. 5(c)**. This procedure is performed for the whole set of simulated particles in order to represent the light regime actually seen by each particle along its travel in the reaction volume. Therefore, the interaction between turbulence and heterogeneity of illumination within a volume was highlighted.

Some microalgal trajectories relatively similar to the one presented in **Fig. 5. (c)** have been reported in previous studies [26], [29], [35], [37]. However, the verification that the database of particle trajectory is correctly sampling the light volume distribution is almost never carried out. Here, we aim to validate the exploitation of light exposure database for the evaluation of growth rates for the different microalgae behaviors mentioned in section 2.1.

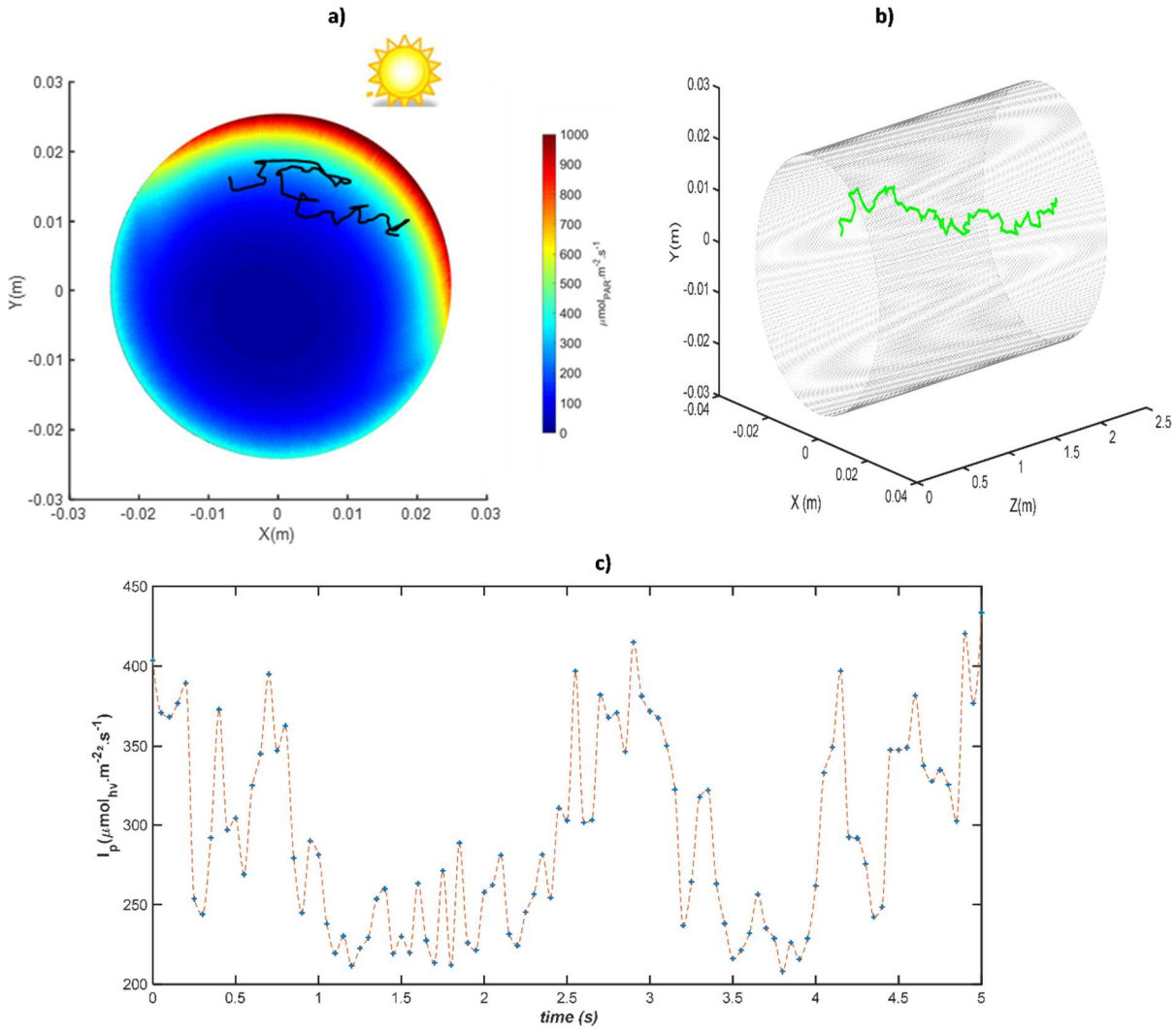

Fig. 5. Followed trajectory of an arbitrary cell for a Re= 20000 and during t= 5(s): (**a**) projection on an irradiation field (2D cross-section), with cell concentration of X=0.9 (g/L), $I_0 = 1241(\mu mol.\, m^{-2}.\, s^{-1})$, diffuse coefficient α=0.4, (**b**) trajectory followed along the longitudinal axis in 3D and (**c**) temporal light intensity recorded during its motion.

3.1.2. Validation of the homogeneous spatial distribution of the cells in the irradiance field

The previously obtained results cannot be validated experimentally nor compared to other simulation studies. Hence, to guarantee the strength of the Lagrangian tracking method (DRW model), it is important to verify that: (i) this procedure ensure a homogeneous spatial distribution of the particles in the volume and (ii) the database generated on light signals recorded by the cells allows a good sampling of the local light intensity values.

First of all, **Fig. 6.** (**a**) shows a uniform spatial dispersion of cells along the tube radius, which is an important result in its own. Indeed, simulations reported in the literature [35] performed with CFD tools by using the standard turbulence model $k-\varepsilon$ coupled to the Lagrangian tracking, overestimate the turbulent kinetic energy in this area and thus generate a numerical bias on the subsequent trajectories' calculation. These methods overestimate the particle concentration in the near walls. In our results, although this artificial buildup exists, due to the lack of the hydrodynamic boundary layer resolution and the insufficient geometric adaptation of the rebound laws, it is however reduced to less than 6% thanks to the particle wall ejection proposed here, which imposes a constraint that forces the cells back into the flow, as described in section 2.3.

Moreover, an "at the point" validation was conducted according to the method described by Gernigon et *al.*, [35] to confirm the uniformity of the distribution of cells in the volume and to analyze the acuity of the near-wall effect. This method consists in comparing the distribution of local light intensities obtained by the spatial irradiance field calculation and the database of light recorded by cells using the stochastic tracking model. This verification approach provides more sound information than an integral approach based on the comparison of the average light available in the volume and the population average obtained by the Lagrangian approach, as has been performed in other studies [26], [36]. In **Fig. 6.** (**b**) the probability density results show that the validation of cell iso-distribution is successful since the irradiance seen by the whole population statistically converges towards the spatial irradiance field in the PBR under given operating conditions (i.e. cell concentration of 0.9 (g/L), I_0=1241($\mu mol.m^{-2}.s^{-1}$), diffuse coefficient α=0.4). Furthermore, it was also verified that the total average irradiation of all the generated data (all particles and all events) corresponds to the irradiance field volume average with less than 2% of relative error between the two values.

(a)

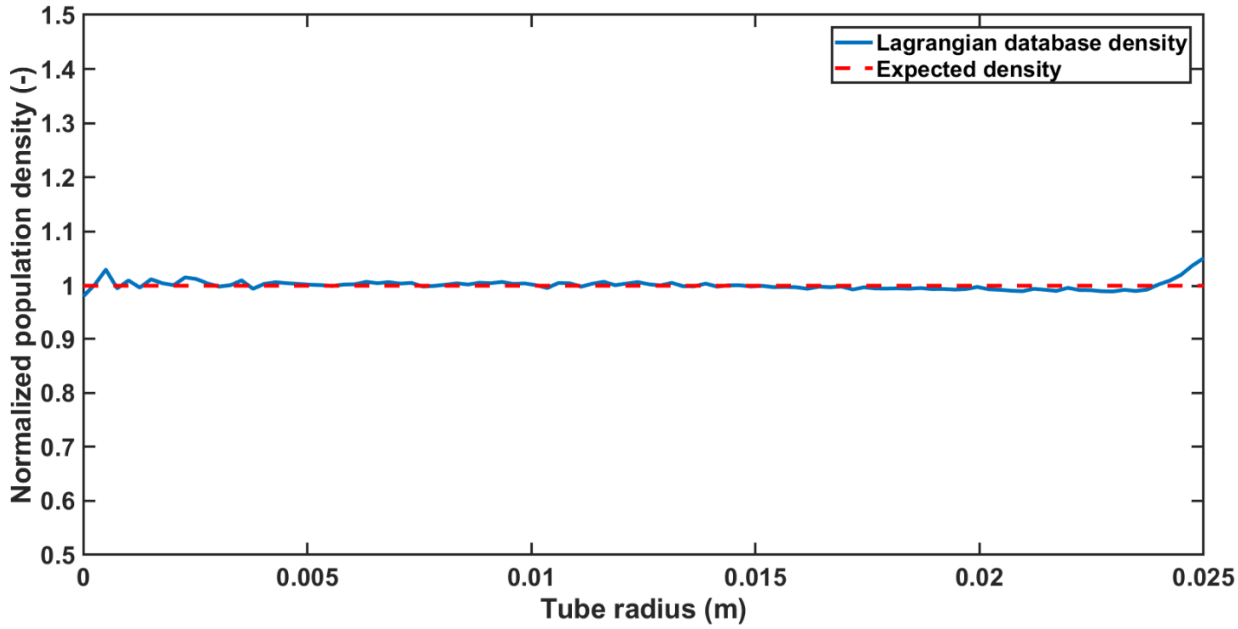

(b)

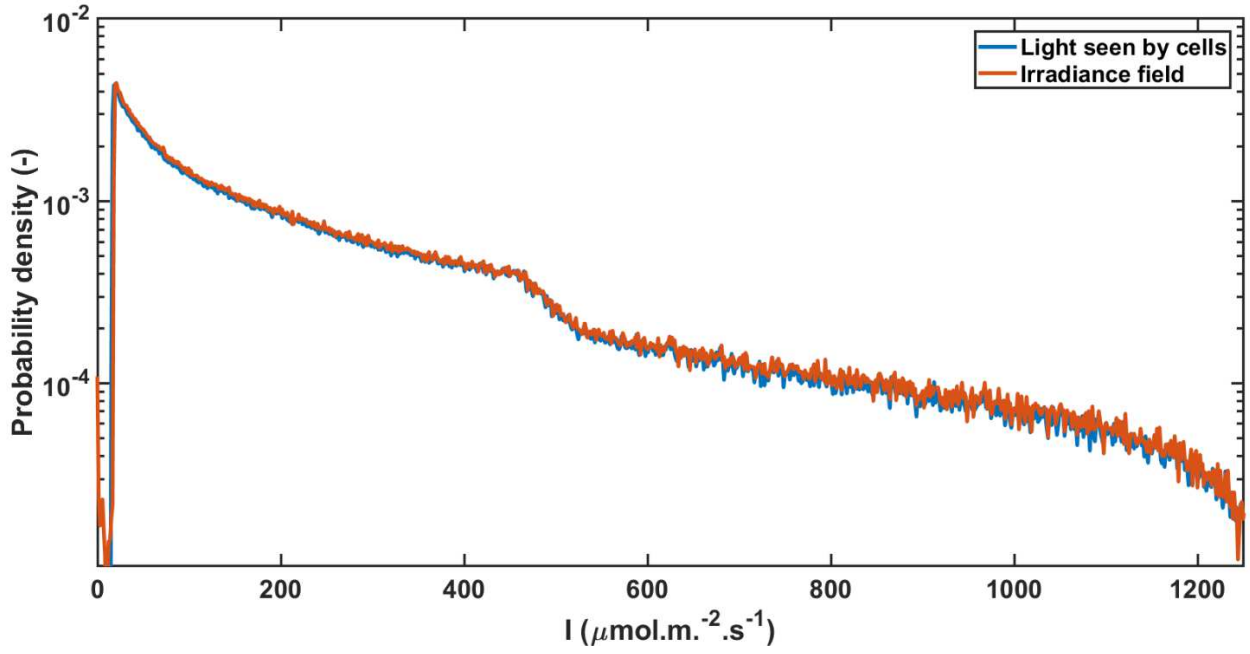

499 **Fig. 6.** (**a**) The radial distribution of the cell population density in the tube, (**b**) Comparison of the irradiance
500 distribution recorded by the cells (using. U_b=0.4 (m/s) corresponding to a Reynold's number of 20000) with
501 light distribution given by the spatial field for cell concentration of X=0.9 (g/L), I_0 =1241($\mu mol.m^{-2}.s^{-1}$),
502 diffuse coefficient α=0.4.

3.1.3. Exposure time distribution in areas close to the wall

Despite small erroneous predictions of particle concentration on the near wall region provided by our particle tracking model, we intend to analyze its impact on the irradiation field integration by the cell population. Indeed, the question that arises here is to know if an overexposure is possible in the zones with very high light intensities causing an eventual inhibition.

To answer this, we need information on the frequency of occurrence of "viscous layer passage" events and their duration. A distribution of the exposure or residence times of all particles is calculated and normalized by the total simulation time, as shown in **Fig. 7**. The shape of this distribution is similar to a decreasing exponential. This latter leads to think of the residence time distribution for a perfectly agitated reactor. Once again, this finding supports the discussion mentioned previously concerning the uniform repartition of the cells in the reactor.

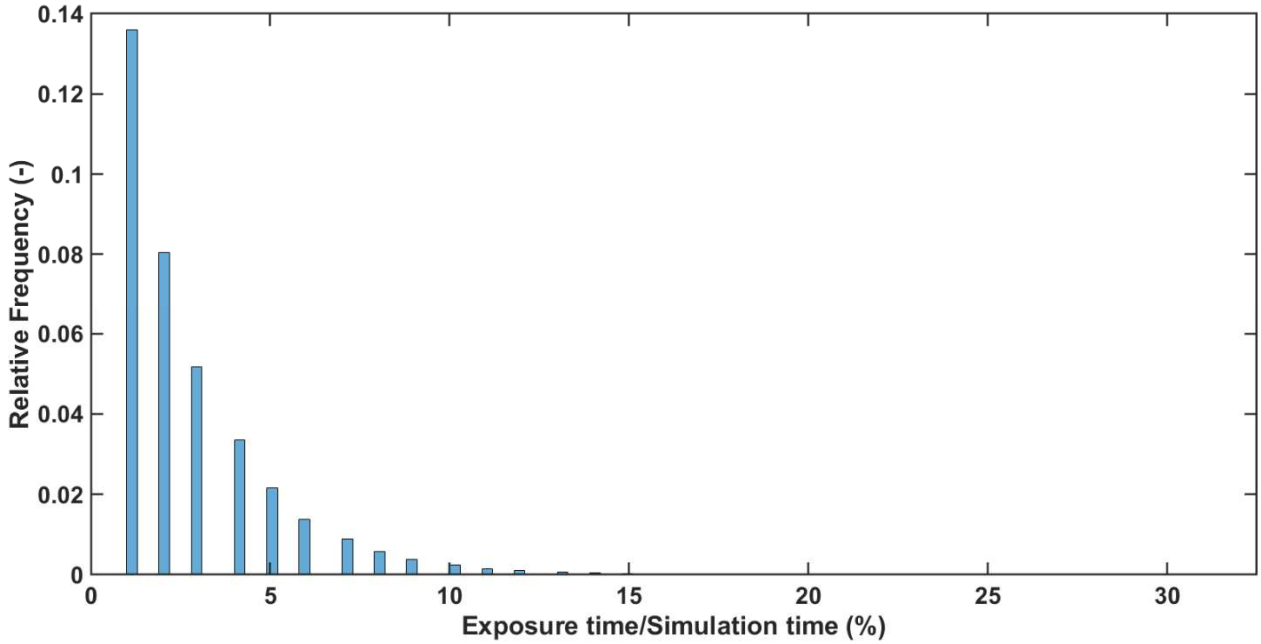

Fig. 7. Distribution of normalized duration of cells exposure to the near-wall layer for the lowest flow velocity value tested in this study (i.e. U_b=0.3 (m/s) corresponding to Re= 15000).

More precisely, these data reveal the passage times of the particles through the entire viscous layer near the reactor walls (a ring of variable thickness according to flow velocity). However, this

boundary layer, can be extremely heterogeneous in terms of light intensities. This heterogeneity increases as the biomass concentration increases.

To our knowledge, there is no consensus on the exact value of the light intensity and the exposure duration that actually cause inhibition of spirulina. According to the experimental data of [28], a period of more than 10s under an irradiance of about 2600 ($\mu mol.m^{-2}.s^{-1}$) is sufficient to have a negative growth rate leading to a total collapse of the culture. These high irradiance intensities are rarely encountered in reality except in subtropical regions. The onset of inhibition under conditions of permanent lighting was also signaled for intensities > 1300 ($\mu mol.m^{-2}.s^{-1}$). With this in mind, we analyzed our light exposure database for whole cells tracked to check the time of cell passage through the very high illuminated zones. To do this we have chosen an extreme operating condition where microalgae could be subject to inhibition (i.e. the highest incident irradiance recorded in Toulouse, France $I_0 = 1402$ ($\mu mol.m^{-2}.s^{-1}$) α=0.33, the lower biomass concentration considered here X=0.3 (g/L), and at the lowest flow velocity tested U_b=0.3 (m/s)). Then, we estimated for each cell the exposure time to irradiances above 1300 $\mu mol.m^{-2}.s^{-1}$. The results plotted in **Fig. 8.** show that the cell switching events to high lights are occasional and of short duration. Thus, this indicates that cells are rather exposed to high intensity flashes of light that are not harmful to growth as opposed to prolonged exposure as in the case of the permanent light regime which causes cell destruction.

The results confirm the harmfulness of such overexposure to light when coupled with the turbulence induced by mixing.

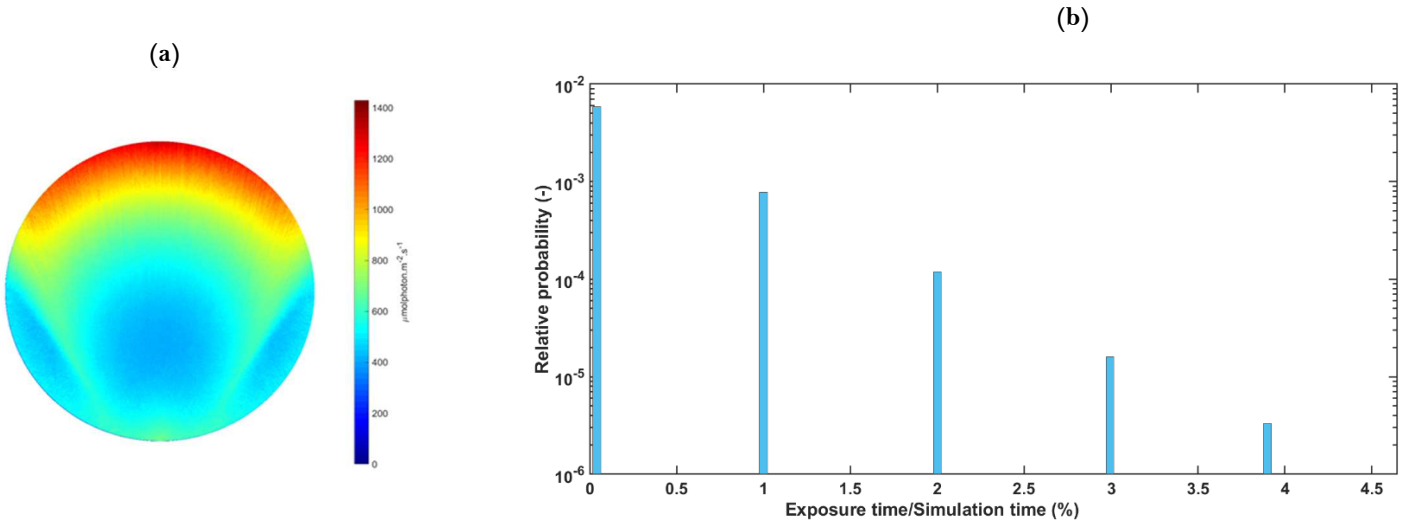

Fig. 8. Light filed with $I_0 = 1402$ ($\mu mol.m^{-2}.s^{-1}$) α=0.33, X=0.3 (g/L), (**b**) Distribution of cell time exposure to inhibitory zones (flow velocity U_b=0.3 (m/s) corresponding to Re= 15000).

3.2. Analysis of growth rate results

3.2.1. Biological dynamic response

The database about the light history of each particle has fed the dynamic model expressed in Eq (7) to obtain the internal variable i evolution that represents the dynamic adaptation of individual cells to the detected light I_p. **Fig. 9** presents the internal variable signal resulting from the biological response to the recorded light fluctuations, for the same cell as in **Fig. 5. (c)**. It was found that the magnitude of strong fluctuations in light exposure is smoothed by the internal variable i due to turbulence induced by hydrodynamic microstructures (i.e. small swirls). This could be explained by the difference in time scales of the hydrodynamic and biological processes: the relaxation time or cell response, τ=0.3 (s), used in the dynamic model, is much greater than the sampling frequency of light exposure and eddy lifetime. Therefore, this allows to filter out the high variations in light exposure, to finally represent only the pattern of fluctuations inferred by the macro-instabilities (i.e. large eddies) of the studied flow.

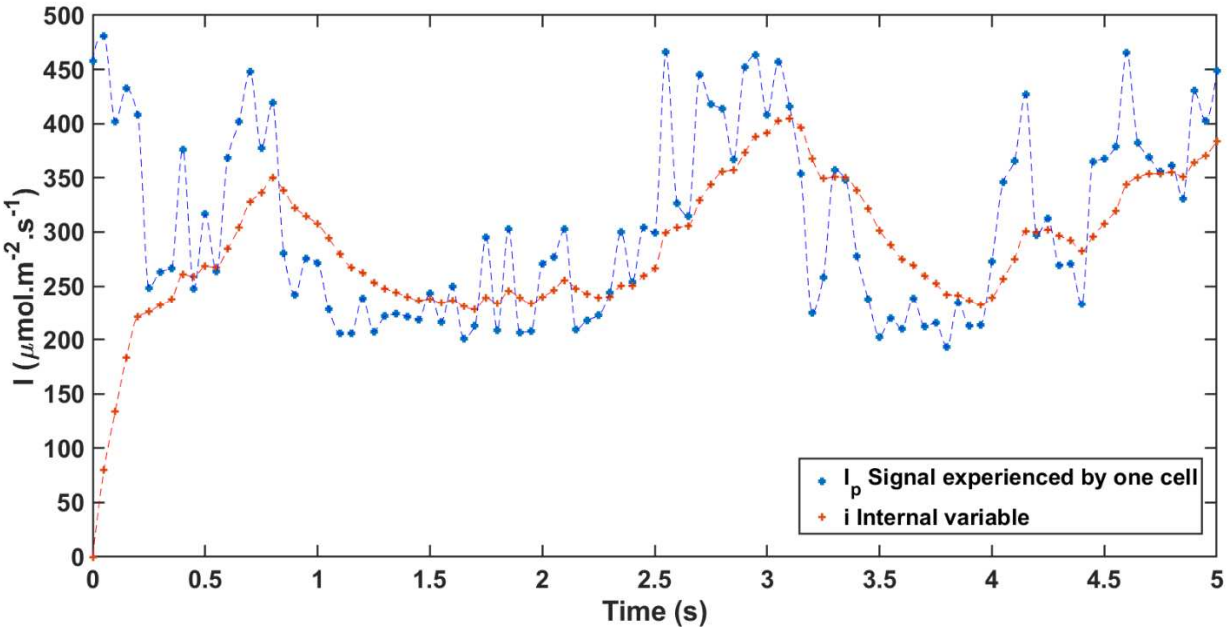

Fig. 9. Dynamic response (red dashed line) of an arbitrary cell to the captured light (blue dashed line) with a characteristic time τ=0.3s using the dynamic model described by [35].

The period and amplitude of the light fluctuations seen by the cells depend on the intensity of the turbulence induced by the fluid hydrodynamics and on the spatial light gradient governed by the biomass concentration and the sunlight energy supplied. The results presented here pertinently reflect the consequence of the combination of the cells light history with a dynamic response kinetic governed by the biological characteristic time. The simulation outcomes for the temporal evolution of the internal variable i constitute a database further used to calculate the global growth rate for a real dynamic biological behavior.

3.2.2. Real growth Kinetics

The PBR overall growth rate were calculated here, according to the modelling approach described in **Fig. 1** in section 2.1, for 10 concentrations between 0.3-1.5 (g/L) and for different liquid flow velocities in the tube U_b (see **Table 2**) expressed in Reynolds number. **Fig. 10** presents the results of the instantaneous response $\mu^a_{V,\tau\to 0}$, the complete integration response $\mu^a_{V,\tau\to\infty}$ and dynamic response with biological adaptation μ^a_V (section 2.1). At low biomass concentrations the growth rates corresponding to the two asymptotic cases and the real case μ^a_V meet together, regardless of the applied flow velocity. This could be explained by the fact that the spatial gradient of light is very

slight which provides to cells the same light exposure, therefore the responses of the microalgae become similar. However, as the biomass concentration increases, the curves become steeper and the overall growth rate diverges according to the behavior of the cells towards the captured light. A deviation of about 60% is recorded at a concentration of 1.5 (g/L) between limit cases (i.e. $\mu^{a}_{V,\tau\to 0}$ and $\mu^{a}_{V,\tau\to\infty}$). In case of the dynamic biological response, the results are positioned between the two asymptotic cases. The mixing or turbulence effect becomes more remarkable with the increase of the biomass concentration since the fraction of dark volumes and light gradient increase. Indeed, as the liquid velocity increases, the growth rates tend toward the maximum limiting case. Simulation results indicate a 20% improvement in PBR performance when the velocity increases from 0.3 (m/s) to 1.68 (m/s) (i.e. Re = 15000 and Re=84000 respectively) for a cell concentration of 1.5 (g/L). This behavior can be explained by the fact that algae filter the fluctuations of light they see and respond to the captured light more slowly than the instantaneous adaptation. Thus, the greater the turbulence, the closer the growth rate is to the upper limit (i.e., the fully integrated case).This beneficial effect of turbulence has also been observed in the experimental results of [82] who recorded a 29% increase in spirulina productivity when the flow regime in a straight tubular PBR switches from laminar to turbulent regime. Indeed, this confirms that the strong turbulence is responsible for the beneficial effects of the strong intermittent exposure of cells at different light intensities in highly heterogeneous spatial gradients. Nevertheless, a too strong turbulence also increases the shear stresses, which must be limited to avoid culture damages. This later effect is not considered in this study.

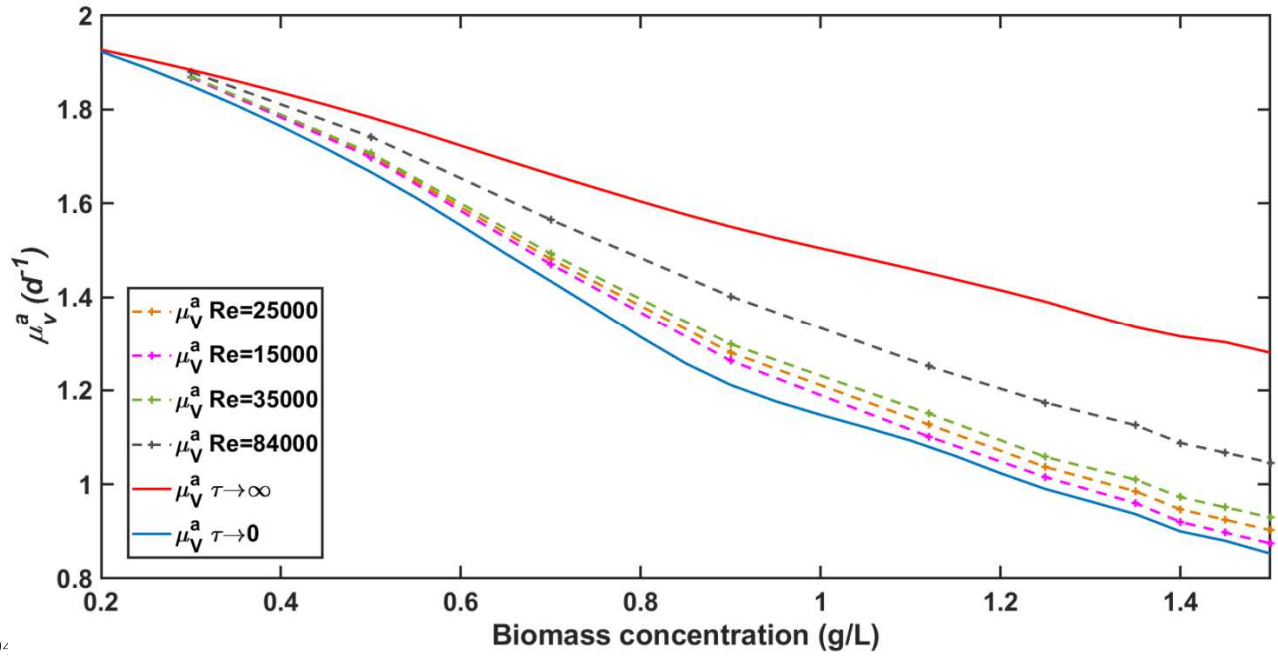

Fig. 10. Influence of turbulence on algae biological growth rate with constant lighting conditions at I_0 =1241($\mu mol.m^{-2}.s^{-1}$), diffuse coefficient α=0.4; response with full light integration (plain red line); instantaneous response (plain blue line); dynamic response with biological adaptation (dashed lines).

3.3.3. Towards a general correlation for the *normalized* specific growth rate Γ

This whole procedure of specific growth rates calculation for both asymptotic and dynamic (real) cases, was performed for a wide range of operating conditions regarding microalgae concentration, flow rate expressed in Reynolds, and received sunlight characteristics (global incident irradiance, direct/ diffuse radiation contribution) in order to cover a wide spectrum of operating possibilities for an outdoor tubular PBR. The *normalized* growth rate Γ was calculated by Eq. (1) for each case simulated.

In other words, Γ translates the capacity of a PBR to reach its optimal performances according to the way the microalgae are exposed to light, which is driven by its operating conditions. Since numerical simulations require a coupling between large databases which is time-consuming, a reduction of the model seems attractive for application cases where PAR performance could be calculated for real operating conditions (i.e., biomass concentration, flow hydrodynamics, lighting quantity and quality).

611 Γ varies between 0 and 1 indicating the efficiency of light use between instantaneous adaptation and
612 full integration. To deeply understand the effect of different operating parameters on PBR ability to
613 drive its performances towards the two asymptotic cases, we started to investigate whether the cell
614 concentration X(g/L) and incident sunlight intensity I_0 affect the rate of light utilization (i.e. Γ) and
615 consequently the real growth rate.

616 At the sight of **Fig. 10**, it is easy to prejudge that the consequence of the biomass concentration on
617 the kinetics is filtered out in the normalization ratio Eq.(1). Hence, to verify this, the corresponding
618 values of Γ as a function of concentration, and for several Reynolds values, were analyzed. The
619 results in **Fig. 11**. **(a)** highlights the independence of Γ to variation of the biomass concentration
620 whatever Reynolds number except at low concentrations where a very slight non-uniformity is
621 observed. This exception could be explained by a better integration of light heterogeneity due to low
622 spatial gradients for low biomass concentrations.

623 **Fig. 11**. **(b)** shows Γ values obtained from simulations of several incident light flux values (in the
624 range of daily and seasonal irradiances) provided by PVGIS [55], for Toulouse, France. At a flow
625 velocity of U_b =0.4 (m/s), Γ is practically constant with an average value of $\Gamma \approx 0.13$, and similar to
626 that shown in **Fig. 11. (a)** for the same Re=20000. The small deviations from the mean observed
627 especially for low irradiances may be explained by the contribution of the diffuse component of
628 sunlight in the calculation of the light fields, which gives the PBR better integration of the light
629 following an additional radial illumination and thus a better exposure of the microalgae to the
630 penetrated light. Following these observations, in addition to the biomass concentration we can
631 already free ourselves from second parameter which is the incident light intensity I_0 for the
632 evaluation of this module Γ. The validation of the independency of $I_0(\mu mol.m^{-2}.s^{-1})$ in the gamma
633 calculation based on literature is detailed in supplementary document (**Appendix** C)

(a)

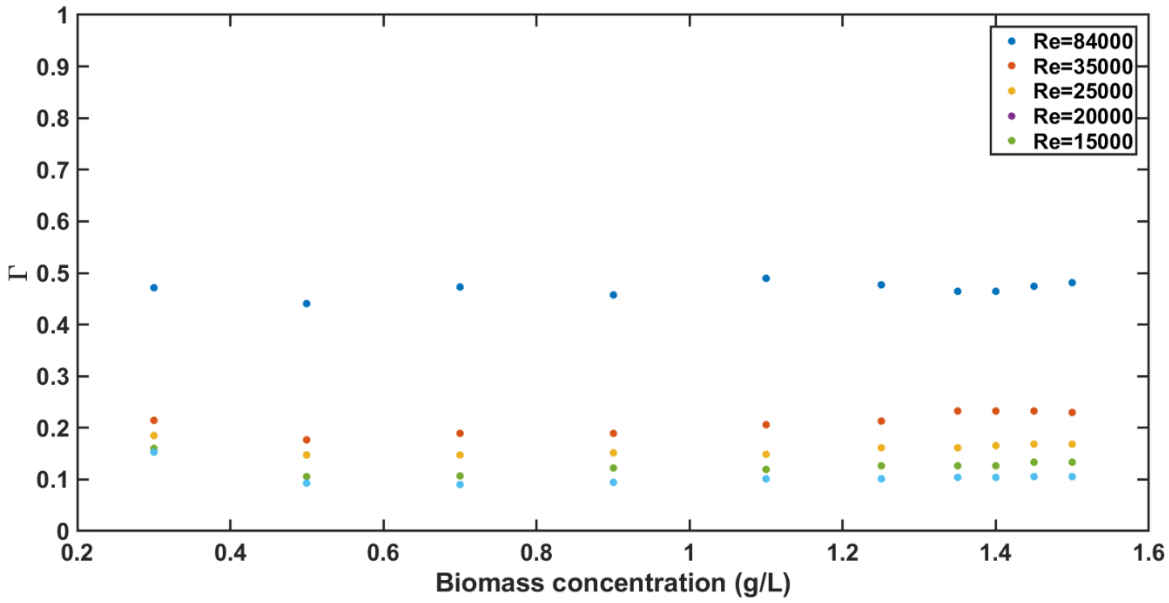

(b)

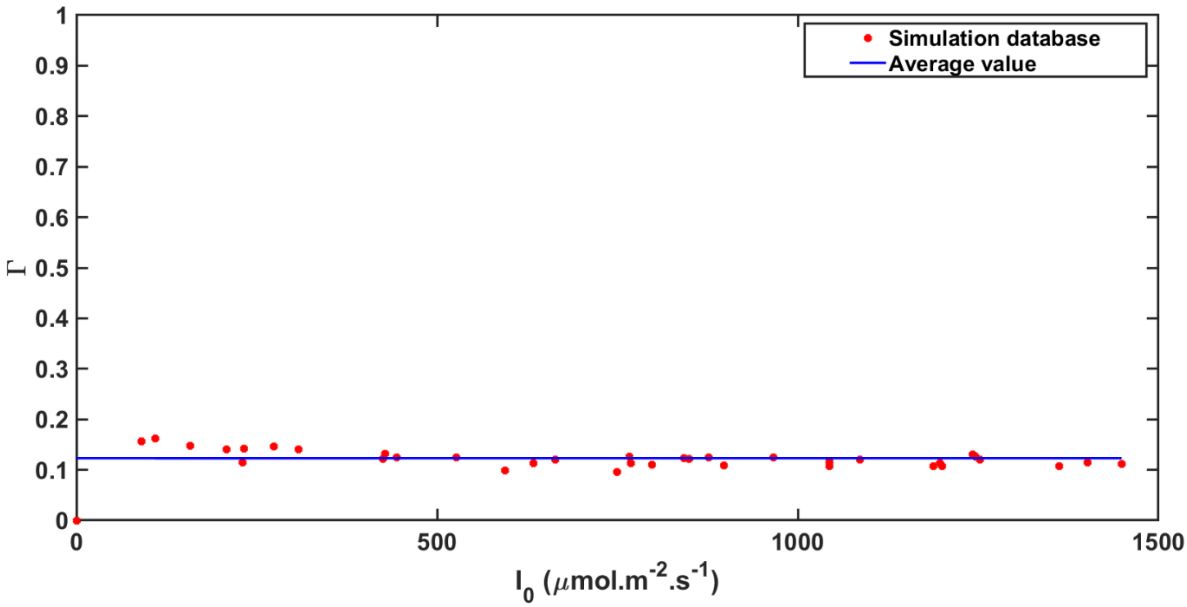

634 **Fig. 11.** Γ values (**a**) as function of biomass concentration X(g/L), (**b**) as function of incident light

635 intensity $I_0(\mu mol.m^{-2}.s^{-1})$ with constant $Re = 20000$.

636 In order to evaluate the effect of turbulence-induced mixing on the ability to improve light

637 utilization, Γ is plotted versus Re **Fig. 12**. Not surprisingly, the value of Γ increases with increasing

638 Re approaching the maximal asymptotic case (i.e. full integration case, when Γ=1). These results

639 confirm again that increased turbulence improves growth rate. Experimental data leading to a

similar conclusion have been documented in the literature [81], [82]: biomass productivity was improved by increasing the flow velocity. This phenomenon can be represented by a linear correlation; however, the acuity of this correlation should be validated for high flow velocities where possible cell damage could occur which implies an upper limit to the flow rate. A total collapse of the culture was also reported in the absence of mixing (low Re <11500) [81], which demonstrates the role of turbulence on the light perceived and used by cells.

Then, this procedure was carried out for four cases of irradiance fields which differs by the contribution of diffuse radiation in the supplied light, represented by the coefficient α. The values of α correspond to the range of the mean ratio of diffuse to global radiation given by PVGIS [55]. **Fig. 12**. highlights the importance of the PBR lighting configuration on the light utilization rate. Indeed, for a given Re number, Γ values are different from one light field to another. Thus, as shown in **Fig. 12.** the higher the fraction of diffuse radiation, which corresponds to a radial irradiation (see section 3.1), the better is the transfer of light into the PBR volume and thus better is the light use by cells. Indeed, in addition to the turbulence induced by the flow velocity of the fluid, the way in which light is brought to the PBR is of major importance in the orientation of the growth kinetics towards the two limit cases.

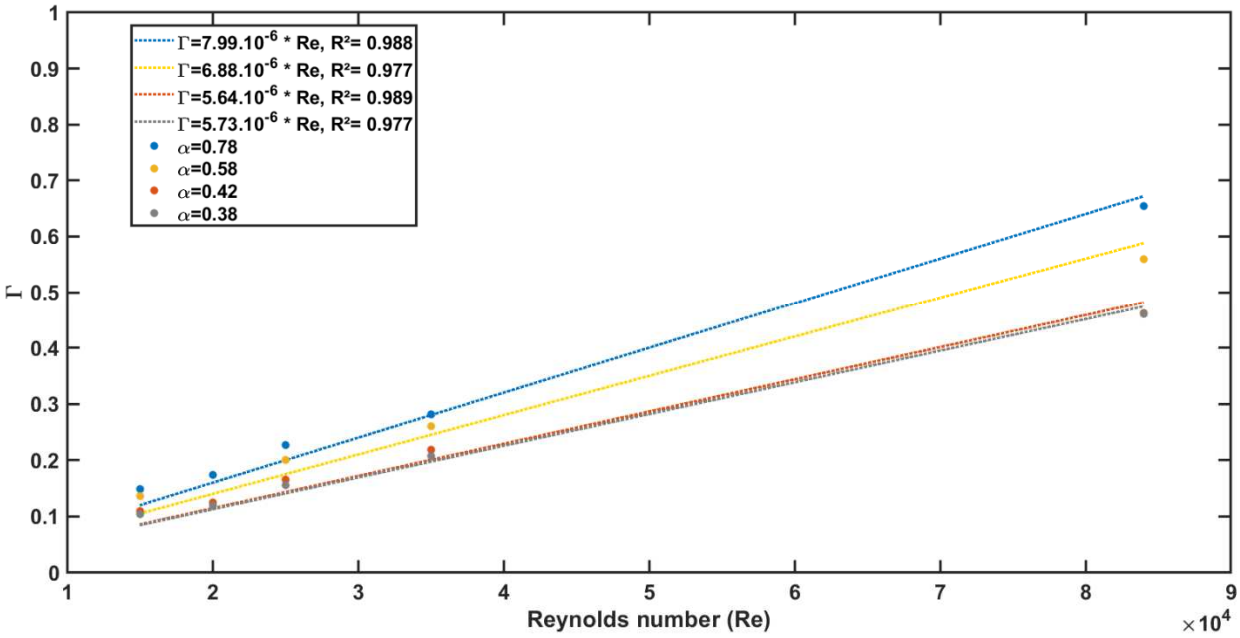

656

657 **Fig. 12.** Γ *vs* Re for different diffuse sunlight fraction α. Round marks represent simulation results.

658 dotted lines represent the correlation Γ= f (Re).

659 To better illustrate the influence of the diffuse radiation on biological growth, the ratio Γ/Re is

660 plotted versus α. in **Fig. 13**. Results showed that, unlike biomass and the intensity of incident light,

661 hydrodynamics coupled with the way in which light energy is supplied to a culture system, has a

662 considerable effect on its ability to use available light. A mathematic expression can be proposed to

663 couple both flow and illumination configuration as follows:

$$\Gamma = 6.19\ 10^{-6} Re\ \alpha + 3.22\ 10^{-6}\ Re \tag{18}$$

664

665 Since Re only varies, in our numerical experiments with the fluid velocity, it's more suitable to write this

666 correlation as function of U_b as follows as the tube diameter D =0.05 (m):

$$\Gamma = 0.31\ 10^{-6} \frac{U_b}{\nu} a + 0.16\ 10^{-6} \frac{U_b}{\nu} \tag{19}$$

667 where ν being the kinematic viscosity of the fluid (m²/s). For Spirulina case, we can suppose $\nu =$

668 10^{-6}(m²/s). So, Γ can be expressed directly as a function of the liquid flow velocity:

$$\Gamma = 0.31\, U_b \alpha + 0.16\, U_b \tag{20}$$

669

670

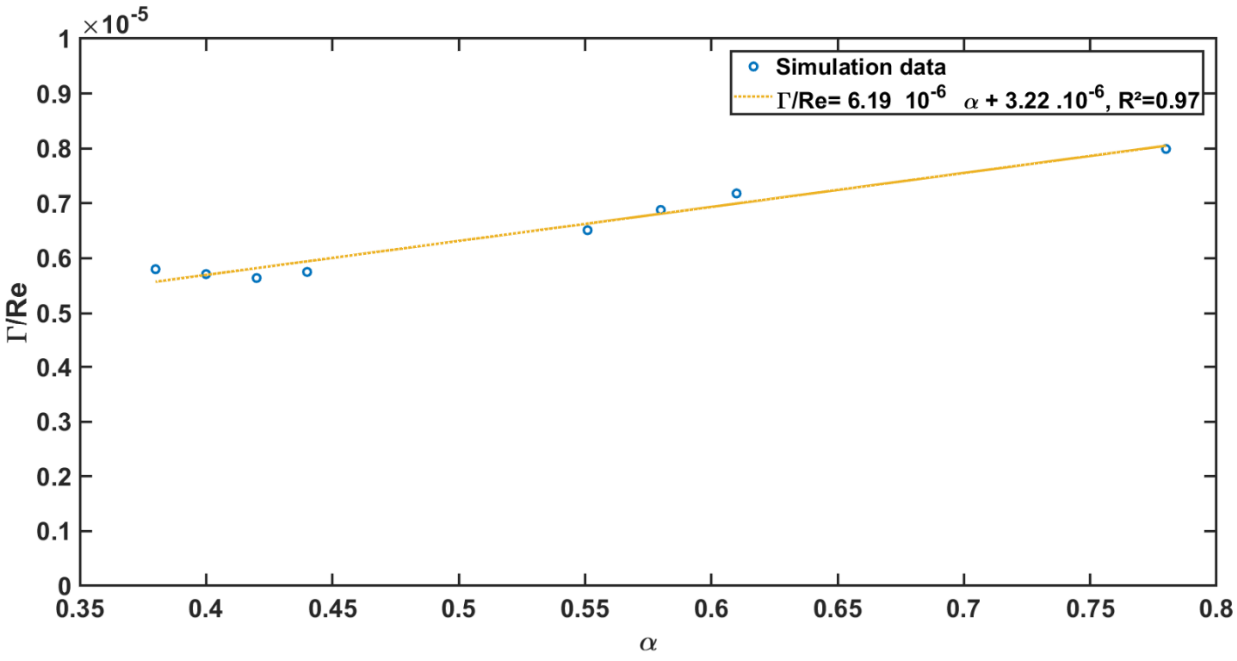

671

672 **Fig. 13.** Effect of the diffuse radiation coefficient α on Γ/Re.

673 From one of the two equations Eq.(19) or Eq.(20) it is possible to predict Γ without having to solve
674 the coupled Monte Carlo light field - hydrodynamic - growth kinetics model. However, to avoid any
675 confusion with the actual performance of the PBR, it is necessary to recall that Γ is an engineering
676 module that describes the skill of the PBR to efficiently expose the cells to the various light
677 fluctuations in its volume, or in other words, the efficiency of light utilization. Therefore, in order to
678 predict the real global growth rate of the solar PBR, a prior estimation of the limit kinetics
679 (instantaneous case and full integration case), relative to a given irradiance field, is required. Indeed,
680 the actual performance is expressed, for each case, using Eq. (18) or Eq. (20) and Eq. (1)

$$\mu_V^a = [(0.31\, U_b \alpha + 0.16\, U_b)\, \mu(\langle \boldsymbol{I} \rangle_V) - \langle \mu(\boldsymbol{I}) \rangle_V] + \langle \mu(\boldsymbol{I}) \rangle_V \tag{21}$$

681

682 The values of μ_V^a calculated by Eq.(8) (i.e. resulting from combination of the three information: the
683 light distribution, the cell motion and biological response time (inertia of the internal variable i)), are
684 compared in **Fig. 14** to the values of μ_V^a predicted by the expression Eq. (21) using Γ's correlation.

685 Although, deviation of 20% between simulated and correlated data (probably due to the small errors
686 made when correlating the link between Γ and turbulence and α), the linear trend is found with a
687 coefficient of determination of R^2 =0.98. The results obtained by Eq.(21) can be considered in
688 sufficient agreement with those obtained using the full modeling approach. Thus, the reliability of
689 using these correlations for an easy estimation of the overall PBR specific growth rate is validated.

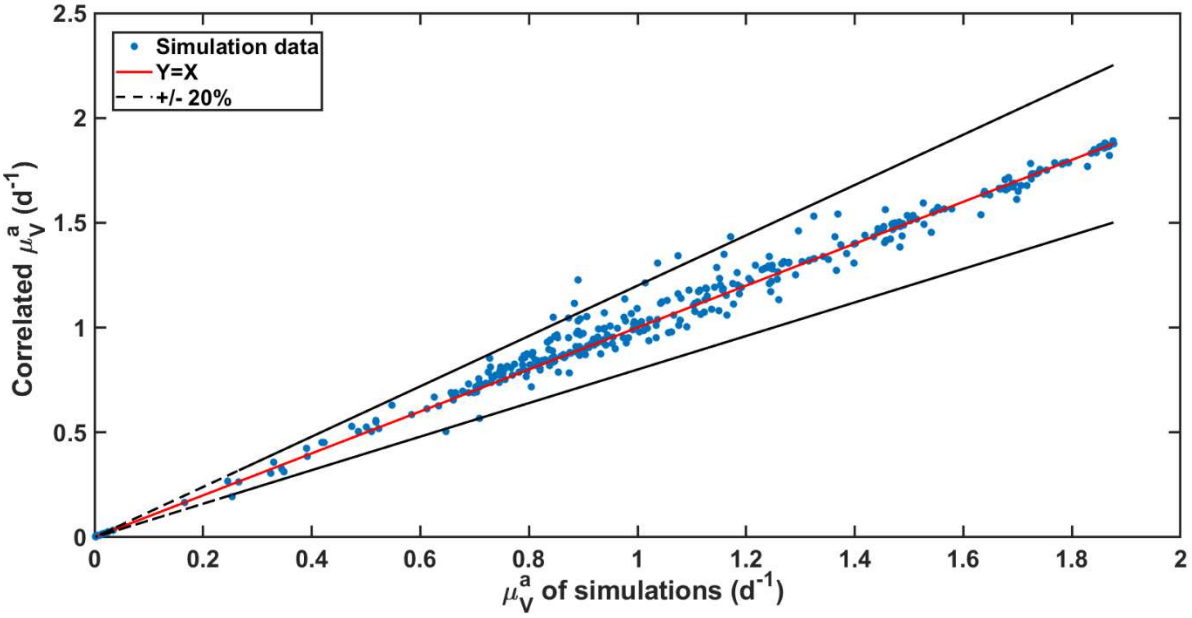

690

691 **Fig. 14.** Comparison between μ_V^a predicated by Eq. (21)and μ_V^a from numerical experiments (from
692 the simulation approach)

693

694 4. Conclusion

695 Through a rigorous modelling of the radiative field considering the solar regime dynamics (i.e. direct
696 light angles and diffuse light contribution), the heterogeneous light structure characterizing a
697 tubular PBR were simulated by a Monte Carlo technique including reflection and refraction on the
698 walls, absorption and scattering by the cells, for 10 biomass concentrations.

Cells trajectories were simulated for five Reynolds number via a Discrete Random Walk model based on turbulent quantities calculated by a $k-\varepsilon$ turbulence model. For the 5 cases, trajectories coupled with the light fields provided the light signals experienced by each of the 1.5×10^5 cells. This database was verified to be representative of the light field inside the PBR. The time resolution (0.05s) is lower than the hydrodynamic and biological time scales involved.

Using a dynamic model based on a biological adaptation of the cells characterized by a response time to temporal fluctuations of the recorded light, the real overall growth rate of the PBR is predicted for 380 cases. The coupling of the flow and light distribution with a dynamic biological model determines the rate of light integration into growth kinetics. Indeed, under a given amount of radiative energy, the real overall PBR growth rate stands between two limit cases that define its extreme theoretical performance.

The *normalized* growth rate Γ translates the PBR's capacity in orienting its real performances towards these limit cases obtained for a given light energy. This concept defines the efficiency of light utilization/integration by biomass circulating in the PBR. Therefore, it depends on the operating conditions and the PBR design including the way the system is subjected to light energy and the quality of the turbulence.

For tubular photobioreactors exposed to the sun, the behavior of the sunlight, as well as the intensity of the turbulence induced by the flow rate (expressed by the Reynolds number), have a combined impact on the ability of the photobioreactor to expose its biomass to the energy received. In order to study the impact of each parameter, a sensitivity analysis was conducted. The results show that this rate of light integration by the PBR cells Γ is independent of biomass concentration variation however it depends entirely on turbulence (i.e., broth flow rate). With respect to light conditions, Γ is not influenced by the variation in intercepted light intensity, but is proportional to the fraction of the scattered radiation that illuminates the entire surface of the PBR.

Hence, a correlation for a fast calculation of Γ was proposed f(Re, α) and it highlights the effect of the PBR design and operation through the inclusion of macroscopic process variables: Reynolds (or implicitly the flow rate) and the light distribution quality at the reactor surface (diffuse light

coefficient). Finally, this correlation was used to predict the real overall PBR growth rate, based on the two asymptotic growth kinetics, which were estimated directly by coupling the irradiance field with the photosynthetic growth model.

Formatting of funding sources

This work was funded by the project READYNOV INSPIRO, EU-FEDER (Fonds Europeen de Developpement Regional), Region Occitanie, France.

References

[1] R. Knuckey, M. Brown, R. Robert, et D. Frampton, « Production of microalgal concentrates by flocculation and their assessment as aquaculture feeds », *Aquac. Eng.*, vol. 35, nº 3, p. 300-313, oct. 2006, doi: 10.1016/j.aquaeng.2006.04.001.

[2] J. A. Del Campo, M. García-González, et M. G. Guerrero, « Outdoor cultivation of microalgae for carotenoid production: current state and perspectives », *Appl. Microbiol. Biotechnol.*, vol. 74, nº 6, p. 1163-1174, avr. 2007, doi: 10.1007/s00253-007-0844-9.

[3] N. Yan, C. Fan, Y. Chen, et Z. Hu, « The Potential for Microalgae as Bioreactors to Produce Pharmaceuticals », *Int. J. Mol. Sci.*, vol. 17, nº 6, juin 2016, doi: 10.3390/ijms17060962.

[4] B. D. Shoener *et al.*, « Microalgae and cyanobacteria modeling in water resource recovery facilities: A critical review », *Water Res. X*, vol. 2, p. 100024, févr. 2019, doi: 10.1016/j.wroa.2018.100024.

[5] C. Posten et C. Walter, *Microalgal Biotechnology: Potential and Production*. Walter de Gruyter, 2012.

[6] A. P. Carvalho, L. A. Meireles, et F. X. Malcata, « Microalgal Reactors: A Review of Enclosed System Designs and Performances », *Biotechnol. Prog.*, vol. 22, nº 6, p. 1490-1506, janv. 2006, doi: 10.1021/bp060065r.

[7] F. Lehr et C. Posten, « Closed photo-bioreactors as tools for biofuel production », *Curr. Opin. Biotechnol.*, vol. 20, nº 3, p. 280-285, juin 2009, doi: 10.1016/j.copbio.2009.04.004.

[8] J. Pruvost, F. Le Borgne, A. Artu, J.-F. Cornet, et J. Legrand, « Chapter Five - Industrial Photobioreactors and Scale-Up Concepts », in *Advances in Chemical Engineering*, vol. 48, J. Legrand, Éd. Academic Press, 2016, p. 257-310. doi: 10.1016/bs.ache.2015.11.002.

[9] B. Wang, C. Q. Lan, et M. Horsman, « Closed photobioreactors for production of microalgal biomasses », *Biotechnol. Adv.*, vol. 30, nº 4, p. 904-912, juill. 2012, doi: 10.1016/j.biotechadv.2012.01.019.

[10] Q. Huang, F. Jiang, L. Wang, et C. Yang, « Design of Photobioreactors for Mass Cultivation of Photosynthetic Organisms », *Engineering*, vol. 3, nº 3, p. 318-329, juin 2017, doi: 10.1016/J.ENG.2017.03.020.

[11] G. A. de Andrade, M. Berenguel, J. L. Guzmán, D. J. Pagano, et F. G. Acién, « Optimization of biomass production in outdoor tubular photobioreactors », *J. Process Control*, vol. 37, p. 58-69, janv. 2016, doi: 10.1016/j.jprocont.2015.10.001.

[12] H. Qiang et A. Richmond, « Productivity and photosynthetic efficiency ofSpirulina platensis as affected by light intensity, algal density and rate of mixing in a flat plate photobioreactor », *J. Appl. Phycol.*, vol. 8, nº 2, p. 139-145, mars 1996, doi: 10.1007/BF02186317.

[13] M. R. Tredici et G. C. Zittelli, « Efficiency of sunlight utilization: Tubular versus flat photobioreactors », *Biotechnol. Bioeng.*, vol. 57, nº 2, p. 187-197, janv. 1998, doi: 10.1002/(SICI)1097-0290(19980120)57:2<187::AID-BIT7>3.0.CO;2-J.

[14] J. Huang, B. Hankamer, et J. Yarnold, « Design scenarios of outdoor arrayed cylindrical photobioreactors for microalgae cultivation considering solar radiation and temperature », *Algal Res.*, vol. 41, p. 101515, août 2019, doi: 10.1016/j.algal.2019.101515.

[15] E. Lee, J. Pruvost, X. He, R. Munipalli, et L. Pilon, « Design tool and guidelines for outdoor photobioreactors », *Chem. Eng. Sci.*, vol. 106, p. 18-29, mars 2014, doi: 10.1016/j.ces.2013.11.014.

[16] J. Pruvost, J. F. Cornet, V. Goetz, et J. Legrand, « Theoretical investigation of biomass productivities achievable in solar rectangular photobioreactors for the cyanobacterium Arthrospira platensis », *Biotechnol. Prog.*, vol. 28, nº 3, p. 699-714, 2012, doi: 10.1002/btpr.1540.

[17] P. M. Slegers, P. J. M. van Beveren, R. H. Wijffels, G. van Straten, et A. J. B. van Boxtel, « Scenario analysis of large scale algae production in tubular photobioreactors », *Appl. Energy*, vol. 105, p. 395-406, mai 2013, doi: 10.1016/j.apenergy.2012.12.068.

[18] P. M. Slegers, R. H. Wijffels, G. van Straten, et A. J. B. van Boxtel, « Design scenarios for flat panel photobioreactors », *Appl. Energy*, vol. 88, nº 10, p. 3342-3353, oct. 2011, doi: 10.1016/j.apenergy.2010.12.037.

[19] L. Pottier, J. Pruvost, J. Deremetz, J.-F. Cornet, J. Legrand, et C. G. Dussap, « A fully predictive model for one-dimensional light attenuation by Chlamydomonas reinhardtii in a

torus photobioreactor », *Biotechnol. Bioeng.*, vol. 91, nº 5, p. 569-582, sept. 2005, doi: 10.1002/bit.20475.

[20] B. Kok, « Photosynthesis in flashing light », *Biochim. Biophys. Acta*, vol. 21, nº 2, p. 245-258, août 1956, doi: 10.1016/0006-3002(56)90004-X.

[21] E. A. Laws, K. L. Terry, J. Wickman, et M. S. Chalup, « A simple algal production system designed to utilize the flashing light effect », *Biotechnol. Bioeng.*, vol. 25, nº 10, p. 2319–2335, 1983.

[22] K. L. Terry, « Photosynthesis in modulated light: Quantitative dependence of photosynthetic enhancement on flashing rate », *Biotechnol. Bioeng.*, vol. 28, nº 7, p. 988-995, 1986, doi: 10.1002/bit.260280709.

[23] S. Abu-Ghosh, D. Fixler, Z. Dubinsky, et D. Iluz, « Flashing light in microalgae biotechnology », *Bioresour. Technol.*, vol. 203, p. 357-363, mars 2016, doi: 10.1016/j.biortech.2015.12.057.

[24] M. Janssen *et al.*, « Efficiency of light utilization of Chlamydomonas reinhardtii under medium-duration light/dark cycles », *J. Biotechnol.*, vol. 78, nº 2, p. 123-137, mars 2000, doi: 10.1016/S0168-1656(99)00233-3.

[25] M. Janssen, J. Tramper, L. R. Mur, et R. H. Wijffels, « Enclosed outdoor photobioreactors: Light regime, photosynthetic efficiency, scale-up, and future prospects », *Biotechnol. Bioeng.*, vol. 81, nº 2, p. 193-210, janv. 2003, doi: 10.1002/bit.10468.

[26] J. Pruvost, J.-F. Cornet, et J. Legrand, « Hydrodynamics influence on light conversion in photobioreactors: An energetically consistent analysis », *Chem. Eng. Sci.*, vol. 63, nº 14, p. 3679-3694, juill. 2008, doi: 10.1016/j.ces.2008.04.026.

[27] X. Wu et J. C. Merchuk, « A model integrating fluid dynamics in photosynthesis and photoinhibition processes », *Chem. Eng. Sci.*, vol. 56, nº 11, p. 3527-3538, juin 2001, doi: 10.1016/S0009-2509(01)00048-3.

[28] S. Xue, Z. Su, et W. Cong, « Growth of Spirulina platensis enhanced under intermittent illumination », *J. Biotechnol.*, vol. 151, nº 3, p. 271-277, févr. 2011, doi: 10.1016/j.jbiotec.2010.12.012.

[29] I. Perner-Nochta et C. Posten, « Simulations of light intensity variation in photobioreactors », *J. Biotechnol.*, vol. 131, nº 3, p. 276-285, sept. 2007, doi: 10.1016/j.jbiotec.2007.05.024.

[30] M. J. Barbosa, M. Janssen, N. Ham, J. Tramper, et R. H. Wijffels, « Microalgae cultivation in air-lift reactors: Modeling biomass yield and growth rate as a function of mixing frequency », *Biotechnol. Bioeng.*, vol. 82, nº 2, p. 170-179, 2003, doi: https://doi.org/10.1002/bit.10563.

[31] A. E. Toninelli, J. Wang, M. Liu, H. Wu, et T. Liu, « Scenedesmus dimorphus biofilm: Photoefficiency and biomass production under intermittent lighting », *Sci. Rep.*, vol. 6, nº 1, p. 32305, août 2016, doi: 10.1038/srep32305.

[32] J. S. Marshall et Y. Huang, « Simulation of light-limited algae growth in homogeneous turbulence », *Chem. Eng. Sci.*, vol. 65, nº 12, p. 3865-3875, juin 2010, doi: 10.1016/j.ces.2010.03.036.

[33] X. Wu et J. C. Merchuk, « Simulation of algae growth in a bench-scale bubble column reactor », *Biotechnol. Bioeng.*, vol. 80, nº 2, p. 156-168, 2002, doi: 10.1002/bit.10350.

[34] X. Wu et J. C. Merchuk, « Simulation of algae growth in a bench scale internal loop airlift reactor », *Chem. Eng. Sci.*, vol. 59, nº 14, p. 2899-2912, juill. 2004, doi: 10.1016/j.ces.2004.02.019.

[35] V. Gernigon, M. A. Chekroun, A. Cockx, P. Guiraud, et J. Morchain, « How Mixing and Light Heterogeneity Impact the Overall Growth Rate in Photobioreactors », *Chem. Eng. Technol.*, p. ceat.201900102, mai 2019, doi: 10.1002/ceat.201900102.

[36] Z.-X. Tong, M.-J. Li, J.-J. Yan, et Z.-L. Gu, « A theoretical analysis of the hydrodynamic influence on the growth of microalgae in the photobioreactors with simple growth kinetics », *Int. J. Heat Mass Transf.*, vol. 158, p. 119986, sept. 2020, doi: 10.1016/j.ijheatmasstransfer.2020.119986.

[37] G. Olivieri, L. Gargiulo, P. Lettieri, L. Mazzei, P. Salatino, et A. Marzocchella, « Photobioreactors for microalgal cultures: A Lagrangian model coupling hydrodynamics and kinetics », *Biotechnol. Prog.*, vol. 31, nº 5, p. 1259-1272, 2015, doi: 10.1002/btpr.2138.

[38] J. S. Marshall et K. Sala, « A stochastic Lagrangian approach for simulating the effect of turbulent mixing on algae growth rate in a photobioreactor », *Chem. Eng. Sci.*, vol. 66, nº 3, p. 384-392, févr. 2011, doi: 10.1016/j.ces.2010.10.043.

[39] J. Pruvost, J. Legrand, P. Legentilhomme, et A. Muller-Feuga, « Simulation of microalgae growth in limiting light conditions: Flow effect », *AIChE J.*, vol. 48, nº 5, p. 1109-1120, 2002, doi: 10.1002/aic.690480520.

[40] J. C. M. Pires, M. C. M. Alvim-Ferraz, et F. G. Martins, « Photobioreactor design for microalgae production through computational fluid dynamics: A review », *Renew. Sustain. Energy Rev.*, vol. 79, p. 248-254, nov. 2017, doi: 10.1016/j.rser.2017.05.064.

[41] J. P. Bitog *et al.*, « Application of computational fluid dynamics for modeling and designing photobioreactors for microalgae production: A review », *Comput. Electron. Agric.*, vol. 76, nº 2, p. 131-147, mai 2011, doi: 10.1016/j.compag.2011.01.015.

[42] P. Hartmann *et al.*, « Growth rate estimation of algae in raceway ponds: A novel approach », *IFAC Proc. Vol.*, vol. 47, nº 3, p. 6216–6221, 2014.

[43] A. Nikolaou, P. Hartmann, A. Sciandra, B. Chachuat, et O. Bernard, « Dynamic coupling of photoacclimation and photoinhibition in a model of microalgae growth », *J. Theor. Biol.*, vol. 390, p. 61-72, févr. 2016, doi: 10.1016/j.jtbi.2015.11.004.

[44] M. Y. Han, Y. H. Park, et T. J. Yu, « Development of a new method of measuring bubble size », in *2nd World Water Congress: Drinking Water Treatment*, vol. 2, London: I W a Publishing, 2002, p. 77–83.

[45] P. H. C. Eilers et J. C. H. Peeters, « A model for the relationship between light intensity and the rate of photosynthesis in phytoplankton », *Ecol. Model.*, vol. 42, nº 3-4, p. 199–215, 1988.

[46] P. H. C. Eilers et J. C. H. Peeters, « Dynamic behaviour of a model for photosynthesis and photoinhibition », *Ecol. Model.*, vol. 69, nº 1, p. 113-133, sept. 1993, doi: 10.1016/0304-3800(93)90052-T.

[47] O. Bernard, « Hurdles and challenges for modelling and control of microalgae for CO2 mitigation and biofuel production », *J. Process Control*, vol. 21, nº 10, p. 1378-1389, déc. 2011, doi: 10.1016/j.jprocont.2011.07.012.

[48] G. Rj, M. Hl, et K. Tm, « Dynamic model of phytoplankton growth and acclimation: responses of the balanced growth rate and the chlorophyll a:carbon ratio to light, nutrient-limitation and temperature », *Mar. Ecol. Prog. Ser.*, vol. 148, p. 187-200, févr. 1997, doi: 10.3354/meps148187.

[49] H. Takache, J. Pruvost, et H. Marec, « Investigation of light/dark cycles effects on the photosynthetic growth of Chlamydomonas reinhardtii in conditions representative of photobioreactor cultivation », *Algal Res.*, vol. 8, p. 192-204, mars 2015, doi: 10.1016/j.algal.2015.02.009.

[50] A. Bernardi, A. Nikolaou, A. Meneghesso, B. Chachuat, T. Morosinotto, et F. Bezzo, « A Framework for the Dynamic Modelling of PI Curves in Microalgae », in *Computer Aided Chemical Engineering*, vol. 37, Elsevier, 2015, p. 2483-2488. doi: 10.1016/B978-0-444-63576-1.50108-4.

[51] P. J. Graham, B. Nguyen, T. Burdyny, et D. Sinton, « A penalty on photosynthetic growth in fluctuating light », *Sci. Rep.*, vol. 7, nº 1, p. 12513, oct. 2017, doi: 10.1038/s41598-017-12923-1.

[52] H. Y. Lee, L. E. Erickson, et S. S. Yang, « Kinetics and bioenergetics of light-limited photoautotrophic growth of Spirulina platensis », *Biotechnol. Bioeng.*, vol. 29, nº 7, p. 832-843, 1987, doi: 10.1002/bit.260290705.

[53] Y.-C. Jeon, C.-W. Cho, et Y.-S. Yun, « Measurement of microalgal photosynthetic activity depending on light intensity and quality », *Biochem. Eng. J.*, vol. 27, nº 2, p. 127-131, déc. 2005, doi: 10.1016/j.bej.2005.08.017.

[54] J. A. Duffie et W. A. Beckman, *Solar engineering of thermal processes / John A. Duffie, William A. Beckman*, 4th ed. Hoboken: John Wiley, 2013.

[55] B. Cattaneo, « Photovoltaic Geographical Information System (PVGIS) », *EU Science Hub - European Commission*, juin 15, 2018. https://ec.europa.eu/jrc/en/pvgis (consulté le oct. 01, 2020).

[56] J. F. Cornet, C. G. Dussap, et G. Dubertret, « A structured model for simulation of cultures of the cyanobacterium Spirulina platensis in photobioreactors: I. Coupling between light transfer and growth kinetics », *Biotechnol. Bioeng.*, vol. 40, nº 7, p. 817-825, 1992, doi: 10.1002/bit.260400709.

[57] J.-F. Cornet, C. G. Dussap, et J.-B. Gros, « Kinetics and energetics of photosynthetic micro-organisms in photobioreactors », in *Bioprocess and Algae Reactor Technology, Apoptosis*, vol. 59, Springer Berlin Heidelberg, 1998, p. 153-224. doi: 10.1007/BFb0102299.

[58] J.-F. Cornet et C.-G. Dussap, « A simple and reliable formula for assessment of maximum volumetric productivities in photobioreactors », *Biotechnol. Prog.*, vol. 25, nº 2, p. 424–435, 2009.

[59] C. A. Arancibia-Bulnes, A. E. Jiménez, et C. A. Estrada, « Development and Modeling of Solar Photocatalytic Reactors », in *Advances in Chemical Engineering*, vol. 36, Elsevier, 2009, p. 185-227. doi: 10.1016/S0065-2377(09)00406-2.

[60] Z. C. Wheaton et G. Krishnamoorthy, « Modeling radiative transfer in photobioreactors for algal growth », *Comput. Electron. Agric.*, vol. 87, p. 64-73, sept. 2012, doi: 10.1016/j.compag.2012.05.002.

[61] A. Brucato, A. E. Cassano, F. Grisafi, G. Montante, L. Rizzuti, et G. Vella, « Estimating radiant fields in flat heterogeneous photoreactors by the six-flux model », *AIChE J.*, vol. 52, nº 11, p. 3882-3890, 2006, doi: 10.1002/aic.10984.

[62] Z. Csogör, M. Herrenbauer, K. Schmidt, et C. Posten, « Light distribution in a novel photobioreactor–modelling for optimization », *J. Appl. Phycol.*, vol. 13, nº 4, p. 325–333, 2001.

[63] V. Rochatte, « Développement et modélisation d'un photobioréacteur solaire à dilution interne du rayonnement », PhD Thesis, UNIVERSITE BLAISE PASCAL -CLERMONT II, 2016.

[64] J. Dauchet, S. Blanco, J.-F. Cornet, M. El Hafi, V. Eymet, et R. Fournier, « The practice of recent radiative transfer Monte Carlo advances and its contribution to the field of microorganisms cultivation in photobioreactors », *J. Quant. Spectrosc. Radiat. Transf.*, vol. 128, p. 52-59, oct. 2013, doi: 10.1016/j.jqsrt.2012.07.004.

[65] G. Marotta, J. Pruvost, F. Scargiali, G. Caputo, et A. Brucato, « Reflection-refraction effects on light distribution inside tubular photobioreactors », *Can. J. Chem. Eng.*, vol. 95, nº 9, p. 1646-1651, 2017, doi: 10.1002/cjce.22811.

[66] J. Hammersley, *Monte Carlo Methods*. Springer Science & Business Media, 2013.

[67] J. Dauchet, « Analyse radiative des photobioréacteurs », PhD Thesis, Université Blaise Pascal, Clermont-Ferrand, 2012.

[68] J.-F. Cornet, C. G. Dussap, J.-B. Gros, C. Binois, et C. Lasseur, « A simplified monodimensional approach for modeling coupling between radiant light transfer and growth kinetics in photobioreactors », *Chem. Eng. Sci.*, vol. 50, nº 9, p. 1489-1500, mai 1995, doi: 10.1016/0009-2509(95)00022-W.

[69] H.-P. Luo et M. H. Al-Dahhan, « Verification and validation of CFD simulations for local flow dynamics in a draft tube airlift bioreactor », *Chem. Eng. Sci.*, vol. 66, nº 5, p. 907-923, mars 2011, doi: 10.1016/j.ces.2010.11.038.

[70] X. Gao, B. Kong, et R. Dennis Vigil, « Comprehensive computational model for combining fluid hydrodynamics, light transport and biomass growth in a Taylor vortex algal photobioreactor: Eulerian approach », *Algal Res.*, vol. 24, p. 1-8, juin 2017, doi: 10.1016/j.algal.2017.03.009.

[71] J. M. J. Toonder et F. T. M. Nieuwstadt, « Reynolds number effects in a turbulent pipe flow for low to moderate Re », *Phys. Fluids*, vol. 9, nº 11, p. 3398-3409, nov. 1997, doi: 10.1063/1.869451.

[72] X. Wu et P. Moin, « A direct numerical simulation study on the mean velocity characteristics in turbulent pipe flow », *J. Fluid Mech.*, vol. 608, p. 81-112, août 2008, doi: 10.1017/S0022112008002085.

[73] J. G. M. Eggels *et al.*, « Fully developed turbulent pipe flow: a comparison between direct numerical simulation and experiment », *J. Fluid Mech.*, vol. 268, p. 175-210, juin 1994, doi: 10.1017/S002211209400131X.

[74] N. Furuichi, Y. Terao, Y. Wada, et Y. Tsuji, « Friction factor and mean velocity profile for pipe flow at high Reynolds numbers », *Phys. Fluids*, vol. 27, nº 9, p. 095108, sept. 2015, doi: 10.1063/1.4930987.

[75] j Laufer, « The structure of turbulence in fully developed pipe flow », *NACA Rep. 1174.*, 1954.

[76] C. J. Lawn, « The determination of the rate of dissipation in turbulent pipe flow », *J. Fluid Mech.*, vol. 48, nº 3, p. 477-505, août 1971, doi: 10.1017/S002211207100171X.

[77] G. I. Taylor, « DIFFUSION BY CONTINUOUS MOVEMENTS », p. 17, juin 1920.

[78] P. Hutchinson, G. F. Hewitt, et A. E. Dukler, « Deposition of liquid or solid dispersions from turbulent gas streams: a stochastic model », *Chem. Eng. Sci.*, vol. 26, nº 3, p. 419-439, mars 1971, doi: 10.1016/0009-2509(71)83016-6.

[79] M. J. Weber, *Handbook of optical materials*. Boca Raton: CRC Press, 2003.

[80] O. Pulz, « Photobioreactors: production systems for phototrophic microorganisms », *Appl. Microbiol. Biotechnol.*, vol. 57, nº 3, p. 287-293, oct. 2001, doi: 10.1007/s002530100702.

[81] E. Molina, J. Fernández, F. G. Acién, et Y. Chisti, « Tubular photobioreactor design for algal cultures », *J. Biotechnol.*, vol. 92, nº 2, p. 113-131, déc. 2001, doi: 10.1016/S0168-1656(01)00353-4.

[82] P. Carlozzi et G. Torzillo, « Productivity of Spirulina in a Strongly Curved Outdoor Tubular Photobioreactor », *Appl. Microbiol. Biotechnol.*, vol. 45, p. 18-23, mars 1996, doi: 10.1007/s002530050642.